Journal of Marine Systems 147 (2015) 29–44

Contents lists available at ScienceDirect

Journal of Marine Systems

journal homepage: www.elsevier.com/locate/jmarsys

Rates of summertime biological productivity in the Beaufort Gyre: A comparison between the low and record-low ice conditions of August 2011 and 2012

Rachel H.R. Stanley [a,*], Zoe O. Sandwith [a], William J. Williams [b]

[a] Woods Hole Oceanographic Institution, 360 Woods Hole Rd., Woods Hole, MA 02543, USA
[b] Fisheries and Oceans Canada, Institute of Ocean Sciences, 9860 West Saanich Road, Sidney, British Columbia V8L 4B2, Canada

ARTICLE INFO

Article history:
Received 11 October 2013
Received in revised form 4 April 2014
Accepted 7 April 2014
Available online 13 April 2014

Keywords:
Arctic Ocean
Canada Basin
Beaufort Gyre
Gross production
Net community production

ABSTRACT

The Arctic Ocean is changing rapidly as the global climate warms but it is not well known how these changes are affecting biological productivity and the carbon cycle. Here we study the Beaufort Gyre region of the Canada Basin in August and use the large reduction in summertime sea ice extent from 2011 to 2012 to investigate potential impacts of climate warming on biological productivity. We use the gas tracers O_2/Ar and triple oxygen isotopes to quantify rates of net community production (NCP) and gross oxygen production (GOP) in the gyre. Comparison of the summer of 2011 with the summer of 2012, the latter of which had record low sea ice coverage, is relevant to how biological productivity might change in a seasonally ice-free Arctic Ocean. We find that, in the surface waters measured here, GOP in 2012 is significantly greater than in 2011, with the mean basin-wide 2012 GOP $= 38 \pm 3$ mmol O_2 m^{-2} d^{-1} whereas in 2011, mean basin GOP $= 16 \pm 5$ mmol O_2 m^{-2} d^{-1}. We hypothesize that this is because the lack of sea ice and consequent increase in light penetration allows photosynthesis to increase in 2012. However, despite the increase in GOP, NCP is the same in the two years; mean NCP in 2012 is 3.0 ± 0.2 mmol O_2 m^{-2} y^{-1} and in 2011 is 3.1 ± 0.2 mmol O_2 m^{-2} y^{-1}. This suggests that the heterotrophic community (zooplankton and/or bacteria) increased its activity as well and thus respired the additional carbon produced by the increased photosynthetic production. In both years, stations on the shelf had GOP 3 to 5 times and NCP 2 to 10 times larger than the basin stations. Additionally, we show that in 2011, the NCP/GOP ratio is smallest in regions with highest ice cover, suggesting that the microbial loop was more efficient at recycling carbon in regions where the ice was just starting to melt. These results highlight that although satellite chlorophyll records show, and many models predict, an increase in summertime primary production in the Arctic Basin as it warms, the net amount of carbon processed by the biological pump during summer may not change as a function of ice cover. Thus, a rapid reduction in summertime ice extent may not change the net community productivity or carbon balance in the Beaufort Gyre.

1. Introduction

The Arctic Ocean is changing rapidly as the global climate warms. Perhaps the most dramatic change in the past decade is the decrease in summertime sea ice extent. Summer sea ice coverage is shrinking (Kwok et al., 2009; Stroeve et al., 2012), with the summer of 2012 setting a new record for the lowest sea ice extent (National Snow and Ice Data Center, 2012). The fraction of multiyear sea ice is decreasing as well; 75% of total ice extent was multiyear ice in the mid 1980s but only 45% was multiyear ice in 2011 (Maslanik et al., 2011). The younger ice that replaces the multiyear sea ice melts more easily leading to increased ice-free areas in the summer. Additionally, the temperature of the Arctic Ocean is increasing, with the Arctic region warming at a rate three times faster than the global mean warming rate (Trenberth et al., 2007). As the climate continues to change, it is likely the Arctic Ocean will experience other changes as well, including changes in freshwater balance (McPhee et al., 2009; Proshutinsky et al., 2009; Yamamoto-Kawai et al., 2009), enhanced permafrost warming leading to increased terrigenous input (Frey and Smith, 2005; Guo and Macdonald, 2006), increased melt season length and delay of freeze-up (Markus et al., 2009), and ocean acidification (Bates and Mathis, 2009; Bates et al., 2009; Mathis et al., 2011; Yamamoto-Kawai et al., 2011).

The Canada Basin is the largest of the four sub-basins of the Arctic. Major changes have been occurring in the Canada Basin (McLaughlin et al., 2011) over the past decade. Summer sea ice extent is decreasing, with warmer ice-free areas and thinner, younger sea ice (Stroeve et al.,

* Corresponding author. Tel.: +1 508 289 2927.
E-mail addresses: rstanley@whoi.edu (R.H.R. Stanley), zsandwith@whoi.edu (Z.O. Sandwith), Bill.Williams@dfo-mpo.gc.ca (W.J. Williams).

http://dx.doi.org/10.1016/j.jmarsys.2014.04.006

2012). The melt season has been lengthening with the onset of freeze-up being delayed (Markus et al., 2009). The Beaufort Gyre is the site of the largest fresh water accumulation in the Arctic, containing about 45,000 km^3 of freshwater (Aagaard and Carmack, 1989). In recent years, there has been an unprecedented increase of fresh water accumulation in the Beaufort Gyre, with a 30% gain in freshwater content between 2003 and 2009 (Proshutinsky et al., 2009). In the low ice year of 2008, freshwater was 60% higher in some areas than climatological values (McPhee et al., 2009). These increases in freshwater content have been accompanied by fresher surface water, a deeper halocline and nitracline, and increased stratification (McLaughlin and Carmack, 2010). Perhaps because of the increased stratification, and thus a reduced summertime vertical nitrate flux (McLaughlin and Carmack, 2010), and/or because of warmer temperatures, the size distribution of phytoplankton has shifted from nanoplankton to picoplankton between 2004 and 2008 (Li et al., 2009). Such shifts in phytoplankton community composition have been predicted to occur as temperatures increase (Falkowski and Oliver, 2007; Moran et al., 2010).

The Arctic Ocean is currently a region of net CO_2 uptake which is disproportionately large for its size — the Arctic Ocean covers only 4% of global ocean area but the CO_2 uptake has been estimated to be up to 14% of global oceanic uptake (Bates et al., 2009). The effect of future changes in sea ice, temperature, and other factors on the CO_2 uptake by the Arctic Ocean is a subject of serious debate. Some studies suggest that CO_2 uptake, at least in parts of the Arctic Ocean such as the Chukchi Sea, will increase (Bates et al., 2011; Fransson et al., 2009). However, other studies predict there will be no net change in CO_2 or even a decrease in CO_2 uptake (Cai et al., 2010) because expected increases in primary production (which would likely lead to increased drawdown of CO_2) will be balanced by rapid re-equilibration with the atmosphere, and increases in temperature and terrigenous runoff. Other studies predict a decrease in CO_2 uptake with climate change because increasing temperature will favor increased rates of respiration (Holding et al., 2013; Kritzberg et al., 2010; Vaquer-Sunyer et al., 2010).

Primary production is one of the factors governing CO_2 uptake and also provides the base energy available for fisheries and other higher trophic levels. Satellite algorithms, specifically tuned for the Arctic, have been used to show that primary production has been increasing as the Arctic Ocean has been warming (Arrigo and van Dijken, 2011; Arrigo et al., 2008a; Brown and Arrigo, 2012; Pabi et al., 2008). These algorithms assume that primary production could not occur in appreciable amounts under sea ice due to light limitation. However, a recent report of a widespread phytoplankton bloom under sea ice (Arrigo et al., 2012) suggests that these satellite algorithms may be grossly underestimating Arctic Ocean primary productivity. If Arctic phytoplankton thrive under sea ice, then a warm and ice-free Arctic Ocean would not necessarily mean a more productive one. Additionally, primary production may increase in some regions, such as the shelf seas (Carmack and Chapman, 2003; Lavoie et al., 2010; Nishino et al., 2011), but decrease in other regions, such as the interior of the Canada Basin (McLaughlin and Carmack, 2010; Nishino et al., 2011) due to nutrient limitation.

In order to predict the future carbon cycle, we need a better understanding of the present-day carbon cycle in the Arctic Ocean. Such an understanding will likely come from a combination of direct observations, remotely sensed products (i.e. primary productivity estimates from tuned satellite algorithms), and ecosystem models. Relatively few direct measurements of productivity have been made in the Arctic. For the most part, measured rates have been of net primary production (NPP = photosynthesis minus autotrophic respiration only) from ^{14}C bottle incubations (e.g. Carmack et al., 2006; Reigstad et al., 2011; Tremblay et al., 2012; Wassmann et al., 2010). NPP has been shown to vary by orders of magnitude depending on season, year and location within the Arctic (Kirchman et al., 2009a). Many fewer studies exist on rates of new production or net community production (Cottrell et al., 2006; Forest et al., 2011; Mathis et al., 2009; Vaquer-Sunyer et al., 2013). If the system is in steady state, then new production should equal net community production (Dugdale and Goering, 1967). In the Amundsen Gulf, an extensive investigation during IPY 2007–2008 (Forest et al., 2011) showed how low sea ice led not only to an increase in gross primary production (Tremblay et al., 2011) but also to increased bacterial production (Nguyen et al., 2012), resulting in relatively little carbon being transferred to higher trophic levels (Forest et al., 2011).

In this study, we used the gas tracers O_2/Ar ratios and triple oxygen isotopes to determine net community production (NCP) and gross oxygen production (GOP) in the Beaufort Gyre region of the Canada Basin in August 2011 and 2012. Net community production is defined as the rate of photosynthesis minus autotrophic and heterotrophic respiration and is a measure of the net carbon taken up by the biological pump. Gross oxygen production is equal to the rate of photosynthetic production and thus represents the energy available at the base of the food chain. By concurrently quantifying NCP and GOP, we separately examine the effect of photosynthesis and respiration. This is important since melting sea ice may not only stimulate photosynthesis but also stimulate respiration through enhanced grazing or bacterial activity and thus result in no net change in the carbon drawdown. Measurements of only NCP could lead to the conclusion that sea ice has no effect on biological productivity, whereas measurements of GOP would suggest that melting sea ice is increasing biological productivity. This may explain the apparent discrepancy in the literature where some studies conclude that primary productivity has not changed significantly in the Arctic (Cai et al., 2010; Grebmeier et al., 2010) while others conclude that biological productivity is increasing (Arrigo and van Dijken, 2011; Arrigo et al., 2008b; Brown and Arrigo, 2012; Pabi et al., 2008).

2. Materials and methods

In this study, we used gas tracers to quantify rates of biological production in the surface ocean. Specifically, we used O_2/Ar to quantify NCP (e.g. Craig and Hayward, 1987; Emerson et al., 1991; Spitzer and Jenkins, 1989) and triple oxygen isotopes to quantify GOP (e.g. Juranek and Quay, 2013; Luz and Barkan, 2000; Luz et al., 1999). O_2 is produced by photosynthesis and consumed by respiration. However, O_2 also responds to physical changes such as thermal forcing and air–sea gas exchange. The noble gas argon has physical characteristics very similar to that of O_2 and therefore can be used as an abiotic analogue of O_2 in order to separate the physical from the biological response (Craig and Hayward, 1987; Emerson et al., 1991, 1993, 1995; Hamme et al., 2012; Juranek and Quay, 2005; Reuer et al., 2007; Spitzer and Jenkins, 1989; Stanley et al., 2010).

The triple oxygen isotope approach rests on the observation that photochemical reactions in the stratosphere fractionate oxygen isotopes in a mass independent way (Lammerzahl et al., 2002; Thiemens et al., 1995). In contrast, on the earth's surface, there is mass dependent fractionation with ^{18}O being fractionated twice as much as ^{17}O. This results in oxygen in the stratosphere having a distinct ratio of ^{16}O:^{17}O:^{18}O. Some of this stratospheric O_2 is mixed into the troposphere and ultimately into the surface water of the ocean. In contrast, phytoplankton produce O_2 from the oxygen in the water molecule in a mass dependent fashion. Thus the triple isotope composition of the dissolved oxygen in water serves as a "made-in tag" — it allows one to quantify what percentage of the oxygen was made by photosynthesis and what percentage was mixed in from air–sea gas exchange. When combined with an estimate of air–sea gas exchange, it serves to quantify GOP (Hendricks et al., 2004, 2005; Juranek and Quay, 2010; Juranek et al., 2012; Luz and Barkan, 2000; Luz et al., 1999; Quay et al., 2010, 2012; Reuer et al., 2007; Stanley et al., 2010).

2.1. Sample collection and analysis

Samples for O_2/Ar and triple oxygen isotope analysis were collected from the Canadian icebreaker *CCGS Louis S. St-Laurent* in the Beaufort Gyre region of the Canada Basin from July 21 to August 18, 2011 and

from August 2 to September 8, 2012, as part of the annual combined Fisheries and Oceans Canada's Joint Ocean Ice Studies (JOIS) and Woods Hole Oceanographic Institution's Beaufort Gyre Observing System (BGOS) expeditions (Fig. 1). At most stations, ~300 mL of seawater was collected from Niskin bottles during standard conductivity–temperature–depth casts into pre-evacuated, pre-poisoned custom-made glass flasks, following the method of Emerson et al. (1999). Samples primarily were collected at a water depth of 6 or 7 m, which was in almost all cases within the surface mixed layer. In 2011, samples were also collected at the deep chlorophyll maximum (DCM) at almost every station. The depth of the DCM was typically between 60 and 80 m. In 2012, only 6 DCM samples were collected. Additionally, at 9 stations in 2011 and 9 stations in 2012, an additional 5 samples were collected within the upper 600 m or in three cases up to an additional 12 samples within the upper 3500 m to investigate the depth distribution of the gas tracers. Samples were collected on both the Canadian and Alaskan Beaufort Shelves and in the Beaufort Gyre region of the deep Canada Basin each year, with one shelf transect in 2011 and two shelf transects in 2012. Exact locations of the samples are shown in Figs. 2–4.

Samples were measured at the Woods Hole Oceanographic Institution on a dual inlet Thermofisher MAT 253 isotope ratio mass spectrometer, largely following the protocol of Barkan and Luz (2003). Modifications to the protocol include: (1) the GC column used was 16 ft in length and held at −3 °C in order to achieve clear and reproducible separation of N_2 and O_2/Ar; (2) all valves used on the processing line were pneumatically actuated stainless steel bellows valves with PCTFE stem tips (Swagelok PN SS-8BK-TW-1C); (3) the cryogenic trap was a custom-made single-sample trap of the design of Lott (2001). A sample was collected on the cryogenic trap at <12 K for 10 min. Then the trap was warmed to 295 K and held at that temperature for at least 5 min. The

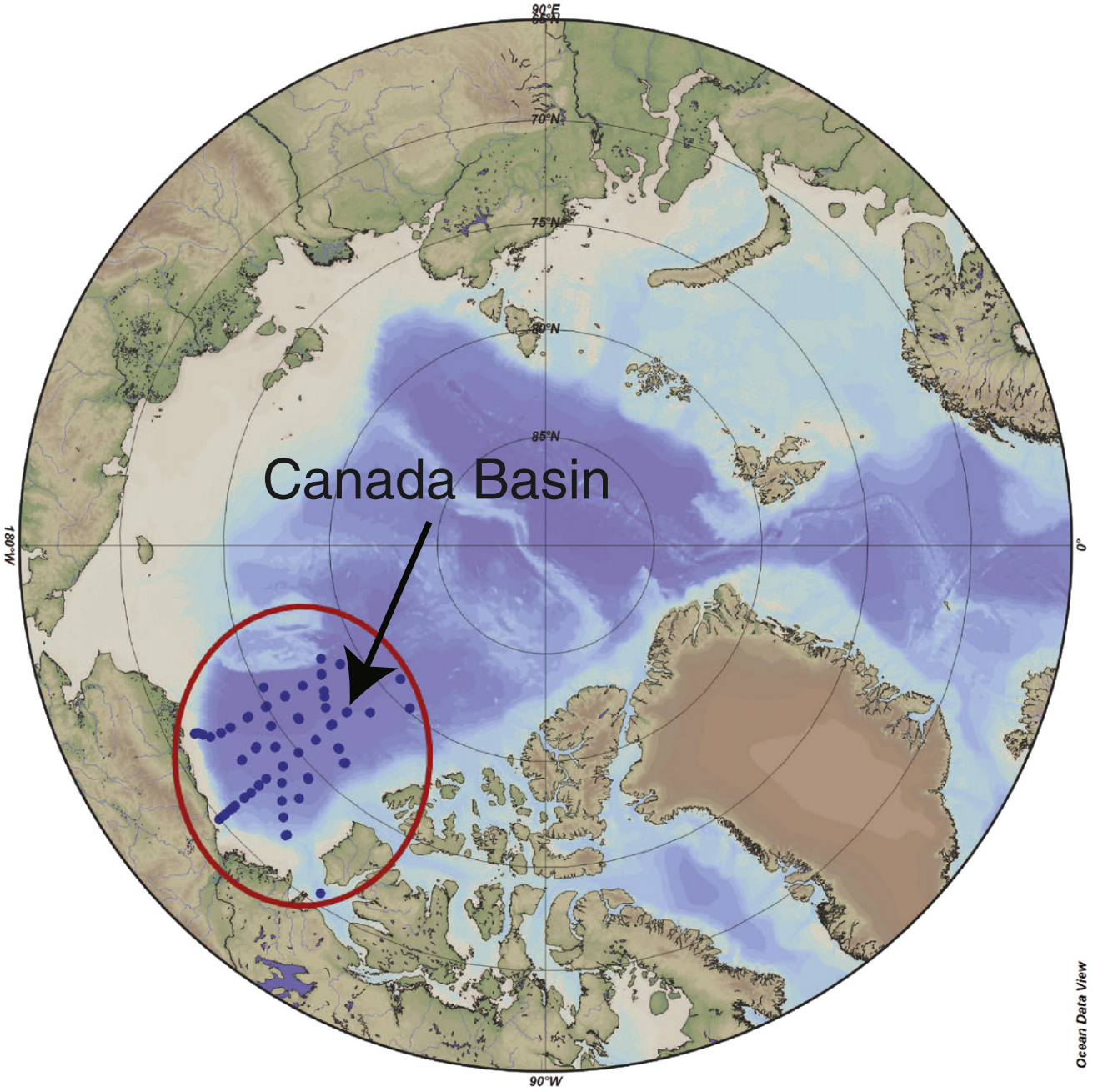

Fig. 1. Map showing the Arctic Ocean, with the Canada Basin, the site of this study, circled in red. The blue dots demarcate the locations of stations occupied in 2011 or 2012, from which triple oxygen isotope and O_2/Ar data for this work was collected. Shading represents bathymetry.

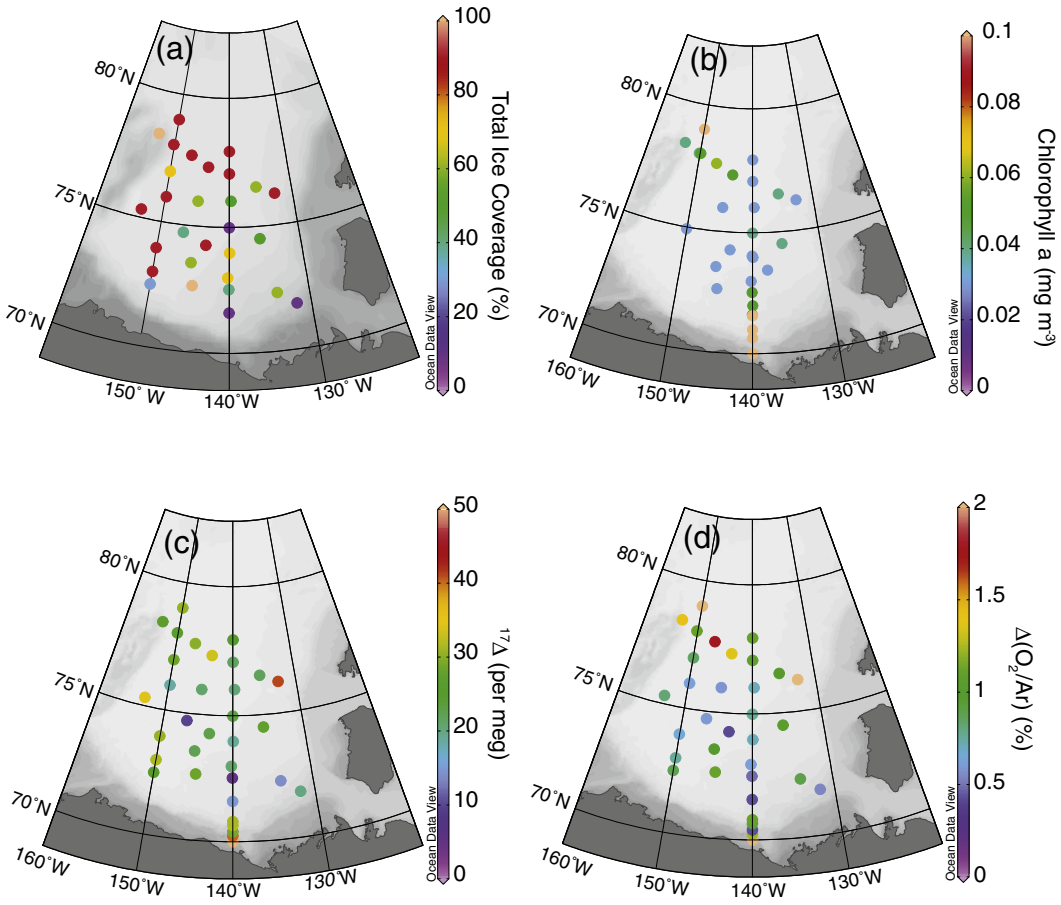

Fig. 2. Measured values of (a) total sea ice coverage (b) chlorophyll a concentrations, (c) the triple isotopic signature of oxygen, $^{17}\Delta$ and (d) the biological saturation ratio $\Delta(O_2/Ar)$ in the Beaufort Gyre region of the Canada Basin in late July and August, 2011. Data is overlain on maps of bathymetry. Sea ice coverage estimates were collected as part of the Ice Watch program (http://www.iarc.uaf.edu/icewatch) by Alice Orlich and Jenny Hutchings.

sample was then expanded directly from the trap into the isotope ratio mass spectrometer where triple oxygen isotopes and O_2/Ar was measured against a custom-made reference gas consisting of 95.5% O_2 and 4.5% Ar (Scott Specialty Gas, custom-order). Clean air, collected at the beach in Woods Hole, MA and stored in an electropolished 2 L stainless steel cylinder, was analyzed after each batch of 10 water samples was analyzed. The oxygen isotope ratios $\delta^{17}O$ and $\delta^{18}O$ where $\delta^{x}O = (({}^{x}O/{}^{16}O)_{smpl} / ({}^{x}O/{}^{16}O)_{ref} - 1) \times 1000$ were calculated with respect to a reference equal to a two week moving average of these air measurements, as is customary. Additionally, one sample of water that had been equilibrated with the atmosphere by stirring in an open 4 L container for at least 2 days in a temperature-regulated laboratory was analyzed alongside every 9 Beaufort Gyre water samples. This was done to (1) ensure integrity of sample processing and analysis and (2) provide accurate measurement of oxygen isotopic ratio of equilibrated water since that term must enter the equations for calculating the rates of GOP from the data.

A measure of the departure from mass dependent fractionation, $^{17}\Delta$, was calculated from $\delta^{17}O$ and $\delta^{18}O$ according to the standard equation of $^{17}\Delta = (\ln(\delta^{17}O/1000 + 1) - 0.5179\ln(\delta^{18}O/1000 + 1)) \times 10^6$. The average $^{17}\Delta$ of equilibrated water samples run during these samples was 7.8 ± 0.7 per meg where the uncertainty reflects the standard error of all water samples analyzed during the time period. The reproducibility of the air standards run during the time period when the 2011 (2012) samples were run is 4.5 (4.7) per meg for $^{17}\Delta$, 0.010 (0.010) ‰ for $\delta^{17}O$, 0.019 (0.016) ‰ for $\delta^{18}O$ and 0.0043 (0.007) for O_2/Ar. The reproducibility of the equilibrated water samples during the time period when the 2011 (2012) samples were analyzed is 5.0 (5.0) per meg for $^{17}\Delta$, 0.011 (0.014) ‰ for $\delta^{17}O$, 0.021 (0.025) ‰ for $\delta^{18}O$ and 0.0078 (0.0063) for O_2/Ar.

Corrections were made to the raw isotope data for the presence of Ar and N_2 in the mass spectrometer, and size of the sample (the latter also being called the differential pressure effect). Corrections for Ar range from −8 to 17 per meg, with undersaturated samples having the largest corrections. The surface samples in particular have a smaller range of corrections, with Ar corrections ranging from 0 to 4 per meg in 2011 and −5 to 0 per meg in 2012. Corrections for N_2 are negligible. Corrections for size range from 1 to 5 per meg. Corrections were determined for $^{17}\Delta$, $\delta^{17}O$, and $\delta^{18}O$ separately.

2.2. Calculations of productivity rates from gas tracer data

GOP (in units of mmol O_2 m^{-2} d^{-1}) is calculated from the measured isotopic ratios according to Eq. (7) of Prokopenko et al. (2011):

$$GOP = kO_{eq}\frac{\frac{X^{17}_{dis}-X^{17}_{eq}}{X^{17}_{dis}}-\lambda\frac{X^{18}_{dis}-X^{18}_{eq}}{X^{18}_{dis}}}{\frac{X^{17}_{P}-X^{17}_{dis}}{X^{17}_{dis}}-\lambda\frac{X^{18}_{P}-X^{18}_{dis}}{X^{18}_{dis}}} \quad (1)$$

where k is the gas transfer velocity (m d^{-1}), O_{eq} is the equilibrium concentration of oxygen, λ is the respiration slope factor = 0.5179, X^{*}_{dis} is the ratio of isotopes $^{*}O/^{16}O$ dissolved in the sample, $X^{*}_{eq.}$ is the ratio of isotopes $^{*}O/^{16}O$ in seawater equilibrated with the atmosphere, and X^{*}_{P} is the ratio of isotopes $^{*}O/^{16}O$ in oxygen produced by photosynthesis

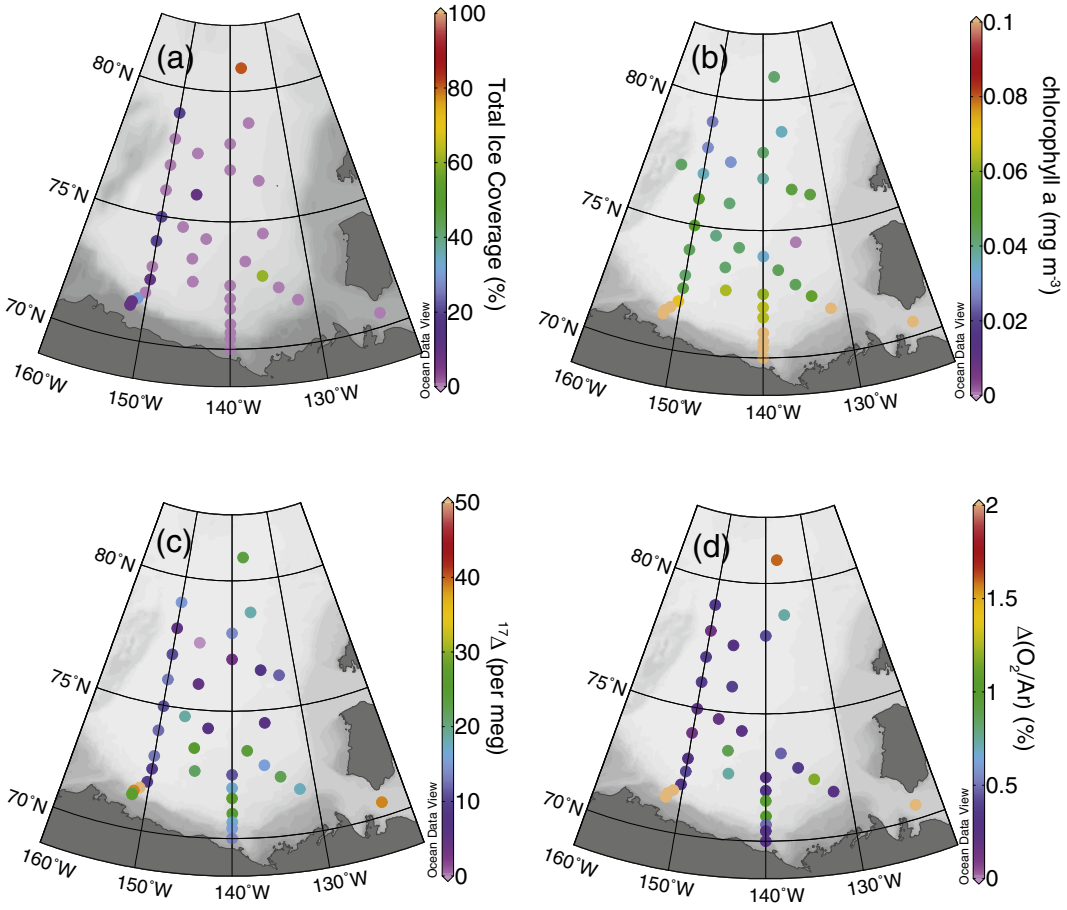

Fig. 3. Data presented in a similar fashion as in Fig. 2 but for measurements made in August and early September, 2012. Thus, the figure displays measured values of (a) total sea ice coverage (b) chlorophyll a concentrations, (c) the triple isotopic signature of oxygen, $^{17}\Delta$ and (d) the biological saturation ratio $\Delta(O_2/Ar)$ in the Beaufort Gyre region of the Canada Basin in August and early September, 2012. Data is overlain on maps of bathymetry.

with * referring to 17 or 18. X* can be calculated from δ* and thus all values are reported here as δ*O and then were converted to X* for use in the equation. The constants used in the equation for the photosynthetic end-member were $\delta^{17}O_P = -10.12‰$ and $\delta^{18}O_P = -20.014‰$ (Eisenstadt et al., 2010; Helman et al., 2005; Luz and Barkan, 2011). For the equilibrated water values, $\delta^{18}O_{eq}$ (in ‰) was calculated according to the equation of Benson and Krause (1984): $\delta^{18}O_{eq} = 0.730 + 427 / (T + 273.15)$ where T is the in situ temperature (K) for that water sample. The $\delta^{17}O_{eq}$ was calculated from $\delta^{18}O_{eq}$ and $^{17}\Delta_{eq} = 8$ per meg. The gas transfer velocity k was calculated as a weighted gas transfer velocity over the previous 60 days, as is done by Reuer et al. (2007), using the gas exchange parameterization of Stanley et al. (2009) and NCEP reanalysis winds (Kalnay et al., 1996; Kistler et al., 2001). No adjustment was made to the gas transfer velocity to account for the presence of ice, due to the uncertainty in how the correction should be made (Else et al., 2013; Fanning and Torres, 1991; Loose et al., 2009, 2011). Thus all the GOP and NCP estimates in partially ice-covered waters are upper bounds. A lower bound estimate could be obtained by multiplying the gas exchange rate by the fraction of open water and thus by extension, multiplying the reported NCP and GOP by the fraction of open water. A discussion of the effect of this simplification is included in Sections 4.1 and 4.3 of this paper. The NCP/GOP ratios are not affected by gas transfer velocity and thus do not suffer from any uncertainty in effect of ice on air–sea gas exchange.

GOP can be converted to gross primary production rates in carbon units by assuming a photosynthetic quotient of 1.2 (Laws, 1991) and a fraction of Mehler reaction of 20% (Bender et al., 1999; Laws et al., 2000), so that gross primary production (C units) = GOP (O_2 units) / $1.2 \times (1 - 0.2)$. Note that all rates represent mixed layer production only and thus do not include any contribution from production below the mixed layer. Significant DCM are observed in the Beaufort Gyre (Hill and Cota, 2005) and thus the rates represented here are likely to be an underestimate of total water column production.

In theory, the estimates of GOP could be overestimating the actual GOP if deeper water with higher $^{17}\Delta$ is being vertically mixed upward. However, the $^{17}\Delta$ just below the mixed layer is not significantly different than mixed layer values on the one station where it was measured. Additionally, there is very strong stratification at the base of the mixed layer (the Brunt–Vaisala Frequency $N = 0.04\ s^{-1}$ to $0.09\ s^{-1}$) in this location, leading to negligible mixing across the base of the mixed layer in the central basin. Thus for most of the data presented, which is from the basin, vertical mixing of water is not likely to bias results.

However, on the shelf, there may be upwelling which could lead to the GOP estimates from the shelf stations being an overestimate, due to upward mixing of higher $^{17}\Delta$ water. Upwelling on the shelf becomes significant about 10 h after easterly winds become greater than $4\ m\ s^{-1}$ (Schulze and Pickart, 2012). Upwelling was likely significant the day before the samples from the shelf stations were collected in 2011 and since the gas tracers average over a few days, it may be biasing the results. The effect of this upwelling would likely be to artificially increase the rates of GOP and decrease the rates of NCP calculated at this station, since $^{17}\Delta$ is elevated and $\Delta O_2/Ar$ is depressed below the mixed layer. We do not have a profile on any of the shelf stations at that year so we cannot calculate the magnitude of the effect. Based on nearby stations, however, it is likely to be small because there usually is not a strong gradient of either gas tracer in the upper 100 m. In 2012,

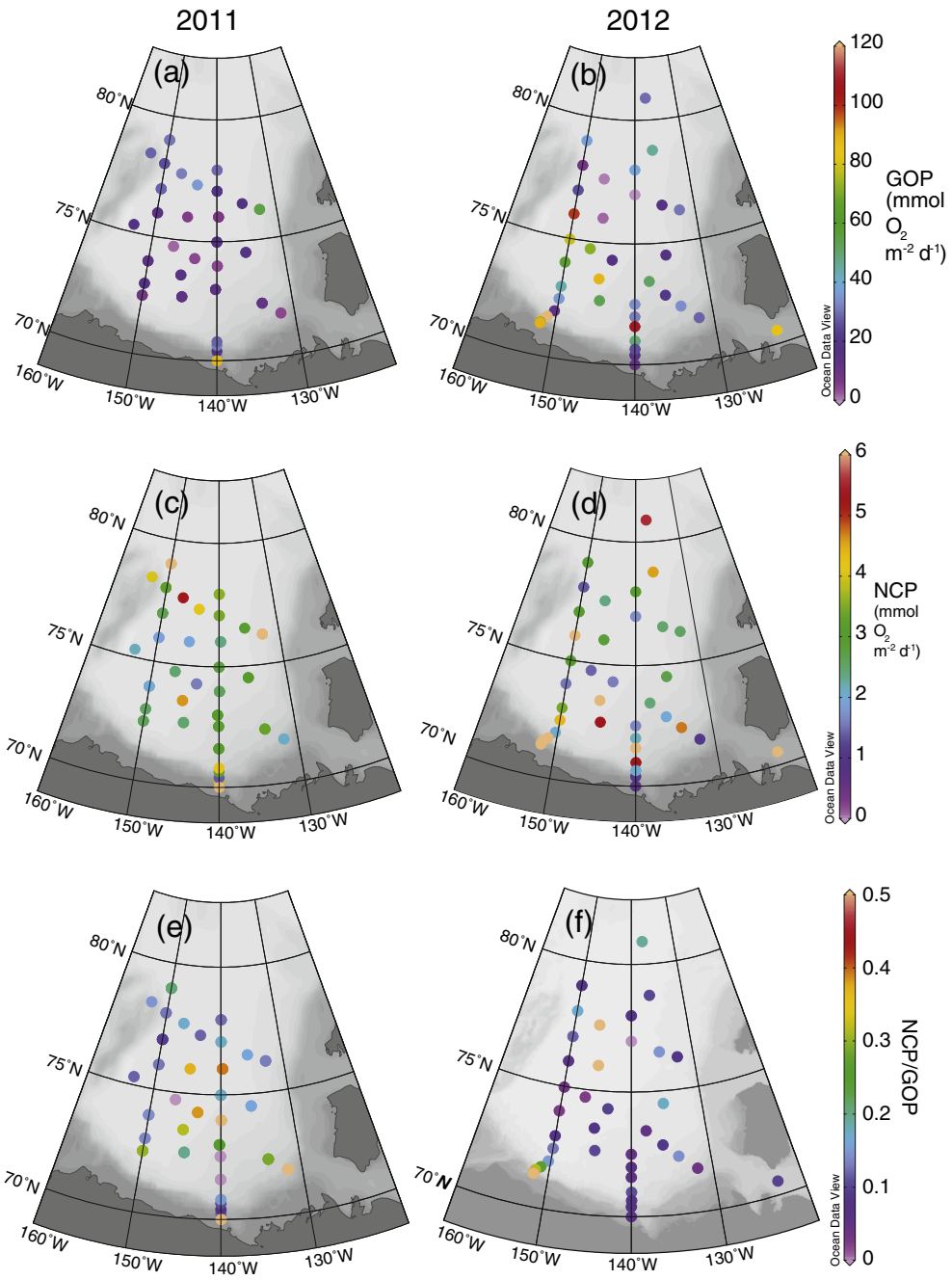

Fig. 4. Rates of gross oxygen production (GOP) determined from triple oxygen isotopic data for the Canada Basin region of the Beaufort Gyre in (a) late July and August, 2011 and (b) August and early September, 2012. Rates of net community production (NCP) determined from the O_2/Ar ratios for the same samples from (c) 2011 and (d) 2012. The ratio of NCP/GOP for the same samples from (e) 2011 and (f) 2012. Some of the rates in the coastal transects are greater than the maximum of the color scales but can be examined in more detail in Fig. 7.

upwelling was probably not significant on the 140°W transect since winds were westerly during sampling and for the preceding week. However, upwelling may be significant for the 151°W transect since winds were westerly during sampling, and southerly for the 48 h prior to sampling, they were easterly prior to that and thus upwelling a few days earlier may still be affecting the gas signature at the time of our measurement (wind data from shipboard winds and NDBC mooring #48211). Profiles from nearby stations, including those on the 140°W transect, suggest that the effect of upwelling would be small since there are only small gradients in the gas tracers in the upper 100 m.

The GOP calculations assume that the time rate in change of $^{17}\Delta$ with time, i.e. $d^{17}\Delta/dt$, is zero — in other words, that the system is at steady-state with respect to triple oxygen isotopes. Ideally, we would have a time-series of $^{17}\Delta$ and would not have to make that assumption but that is rarely the case in oceanographic studies. We expect the error introduced by this assumption to be small because we have used satellite data (see Section 4.5) to confirm that the cruise is not in the middle of bloom conditions, which might have rapidly changing $^{17}\Delta$. Modeling studies have shown that as long as one is not in bloom conditions and entrainment does not significantly affect the $^{17}\Delta$ (and the strong stratification that was set well before the cruise occurred makes entrainment unlikely), the simple steady-state assumption typically leads to uncertainties of <20% in the GOP estimates (Nicholson et al., 2014). Additionally, if there are non-bloom conditions (as in this study), then the errors due to the time rate of change term often cancel out when GOP is being calculated on a regional average. So our conclusions on any one data-

point may have an error of 20% but the error on the average of the rates in the Canada Basin in a given year probably have much smaller error due to the steady state assumption.

NCP is calculated from O_2/Ar by assuming steady state and negligible effects of horizontal and vertical mixing. The shallow mixed layers in the region (typically ~10 m) lead to the integration time of the tracers being only a few days. The assumption of small changes in productivity over several days is likely reasonable in most cases but may not hold in the marginal ice zone. As described above for triple oxygen isotopes, the time rate of change assumption likely leads to small errors, especially when averaging over the entire Canada Basin. In an O_2/Ar modeling study, it has been shown that regional averages are less affected by errors from the steady-state assumption than individual points (Jonsson et al., 2013). Additionally, the strong stratification (the Brunt–Vaisala Frequency N = 0.04 s^{-1} to 0.09 s^{-1}) at the base of the mixed layers makes vertical mixing negligible in the central basin. On the shelf transects, however, upwelling may be occurring which could be leading to the NCP and GOP estimates being an overestimate. The effect of upwelling on NCP in the shelf transects was described above, in the section on GOP calculation.

ΔO_2/Ar is defined as $(O_2/Ar)_{meas} / (O_2/Ar)_{eq.} - 1$ and NCP is calculated (e.g. Hendricks et al., 2004), in units of mmol O_2 m^{-2} d^{-1} as

$$NCP = kp[O_2]_{sat}\Delta(O_2/Ar) \quad (2)$$

where k is the gas transfer velocity, calculated as described in the previous paragraph, and ρ is the density of water as calculated by Millero and Poisson (1981).

The NCP/GOP ratio, which is a measure of how tightly a system is recycling carbon, can be determined as the ratio of the above-calculated NCP and GOP values or if one assumes steady state, they can be estimated by the ratio of the gas tracers, such that

$$\frac{NCP}{GOP} = \rho\Delta(O_2/Ar)\frac{{}^{17}\Delta_{smple} - {}^{17}\Delta_{photo}}{{}^{17}\Delta_{eq} - {}^{17}\Delta_{smple}} \quad (3)$$

where ${}^{17}\Delta_{smple}$ is the measured triple oxygen isotopic ratio of the sample, ${}^{17}\Delta_{photo}$ is the triple oxygen isotopic value of O_2 produced by photosynthesis = 249 per meg, and ${}^{17}\Delta_{eq}$ is the triple oxygen isotopic value of equilibrated water (8 per meg). The two methods differ only slightly in this location, presumably due to the steady state simplification not completely holding. All results reported here are for the NCP/GOP ratio being calculated directly from NCP and GOP values.

2.3. Ancillary data

Visual sea ice observations were collected as part of the Ice Watch program (http://www.iarc.uaf.edu/icewatch). To that end, total ice cover was estimated by trained ice observers on the bridge of the ship at hourly intervals along the cruise track as well as at arrival on each station. Ice concentration, ice type (whether first year or multi-year ice) and partial concentration of each type were recorded using Antarctic Sea Ice Processes and Climate (ASPeCt) conventions (Worby and Alison, 1999) within 3 nautical miles of the ship. The concentration data is estimated in tenths. Stage of melt of the ice was recorded following standard Russian conventions (Vasilly Smolyanitsky, personal communication), which follow World Meteorological Organization nomenclature (WMO, 1989), whereby ice is classified in 5 stages of melt that range between surface wetting and rotten ice. The presence of melt ponds was recorded and melt pond coverage of the ice was estimated in tenths. Photographic records from two webcams mounted on the ship as well as hourly photographs taken by the ice observers were used to check the bridge observations. In 2012, the Ice Watch program did not make visual sea ice observations at every station. Thus we used ice estimates made by a scientist onboard the ship (but not necessarily a trained ice observer) who observed the ice just before the CTD cast. On the many occasions when there were estimates from both the Ice Watch program and the cast estimates by the scientists, they agreed quite well. Additionally, the Ice Watch program, as well as estimates of ice thickness made from satellite passive microwave concentration, all agree that 2012 had very little sea ice compared to 2011.

Chlorophyll-a concentrations were determined from water collected from Niskin bottles that had been immediately filtered at 0.7 μM through GF/F 25 mm filters. Concentrations of nutrients, including phosphate, were determined from samples collected from Niskin bottles. The filters were stored at −80 °C until analysis by fluorometry, which occurred within one month from returning from sea. Precision based on duplicate samples was 0.01 μg L^{-1} and detection limit was 0.025 μg L^{-1}.

Samples for phosphate were collected from unfiltered water from Niskin bottles. Analysis was typically performed within 24 h by a nutrient autoanalyzer, as described by McLaughlin et al. (2008). If storage was required for more than 24 h, samples were stored at 4 °C. The precision based on measurement of standards was 0.015 mmol m^{-3}. Detection limit was 0.006 mmol m^{-3}.

Mixed layer depths were calculated at the stations from CTD density profiles using a criterion of a density difference of 0.1 kg m^{-3} between the surface and the depth of the mixed layer. Temperature and salinity were determined from the CTD system (seabird SBE9+), which had two temperature sensors (SBE3 plus) and two conductivity sensors (SBE 4C). The second pair of sensors is used if there are problems with the primary sensors. Salinity measured in bottle samples using an autosalinometer (Guildline Autosalinometer, model 8400B) was used to calibrate the primary CTD salinity sensor. Precision for these bottle salinity samples based on duplicated samples measured repeatedly was 0.003. Accuracy based on running IAPSO standard seawater (batch P152) was 0.0015. Density was calculated from salinity and temperature data from the primary sensors according to Millero and Poisson (1981).

Satellite productivity estimates for the locations of the data were interpolated from daily maps produced by an algorithm designed especially for the Arctic Ocean (Arrigo and van Dijken, 2011; Pabi et al., 2008). The estimates were made based on MODIS/Aqua chlorophyll (Level 3, binned, 8 day). When estimates did not exist for locations near the sampling stations due to presence of clouds or sea ice no satellite productivity was assigned. Thus the number of stations where satellite productivity estimates is reported is smaller than the number of stations where gas tracer rates are determined.

3. Results

Maps of total ice coverage, mixed layer chlorophyll concentrations, mixed layer ${}^{17}\Delta$, and mixed layer ΔO_2/Ar for 2011 (Fig. 2) and 2012 (Fig. 3) show distinctive patterns. In 2011, total ice coverage is highest on the northern and western edges of the sampling grid. Chlorophyll concentrations are much larger in the shelf stations than in the open basin and are slightly elevated in the northwest corner of the sampling grid, where ice coverage is high. However, they are not elevated under the other regions where ice coverage is still high. ${}^{17}\Delta$ is also highest on the shelf stations and is slightly higher on the northern and western edges of the sampling grid. $\Delta(O_2/Ar)$ is not much different in the shelf stations than in the basin stations with the exception of the nearest to shore shelf station. $\Delta(O_2/Ar)$ is higher on the N edge of the grid but not on the W edge of the grid.

In 2012, there was virtually no sea ice in the entire grid. Surface chlorophyll concentrations in the basin are higher in 2012 ($Chl_{2012,avg}$ = 0.07 ± 0.01 mg m^{-3}, excluding shelf stations) than in 2011 ($Chl_{2011,avg}$ = 0.04 ± 0.01 mg m^{-3} excluding shelf stations). Unless otherwise noted, all uncertainties listed in this paper are equal to the standard error of the average of the rates within the region. In 2012, like in 2011, the highest chlorophyll values were in the coastal transects. Indeed, the shelf chlorophyll averages 0.36 ± 0.1 mg m^{-3},

which is a factor of 6 larger than the basin average chlorophyll concentrations. In 2012, $^{17}\Delta$ and $\Delta(O_2/Ar)$ are highest in the shelf transect along 151°W; however, the shelf transect along 140°W has much smaller $^{17}\Delta$ and $\Delta(O_2/Ar)$ than in 2011.

$^{17}\Delta$ and $\Delta(O_2/Ar)$ reflect a combination of productivity and gas exchange since productivity increases the tracer signal in the surface water and gas exchange erodes it. Thus to fully compare one year and another, or between one station and another, it is important to compare NCP and GOP rather than the gas tracers themselves. Thus in Fig. 4, NCP, GOP, and the NCP/GOP are presented for 2011 and 2012. GOP is larger in 2012 than in 2011. The basin average, i.e. excluding shelf stations, for GOP in 2012 = 38 ± 3 mmol O_2 m^{-2} d^{-1} whereas in 2011, the basin average GOP = 17 ± 5 mmol O_2 m^{-2} d^{-1}. The uncertainties given above are the standard error of the basin samples for that year (i.e. excluding coastal transects). The uncertainty on any given rate measurement is approximately 30% and is set by a combination of uncertainty in the measurement of $^{17}\Delta$ (5 to 8 per meg) and uncertainty in the gas exchange estimate (20%). Since the measurement uncertainty is a constant number, regardless of sample size, the total uncertainty due to the measurements ranges from ~20% to 30% for the samples with low $^{17}\Delta$ values, and thus low GOP rates, to 10% for the samples with high $^{17}\Delta$ values and thus high GOP rates. Since the measurement uncertainty is randomly distributed, it does not bias the averages. However, the additional ~20% uncertainty due to air–sea gas exchange may have a bias in one year vs. another. The uncertainty in air–sea gas exchange in the presence of ice would lead to our 2011 estimates being an overestimate of GOP. Despite this potential overestimate, the fact that the 2011 rates are still well below the 2012 rates implies that the conclusion of significantly higher GOP in 2012 than in 2011 is robust.

The locations where GOP was measured in 2012 are not exactly the same as the locations where GOP was measured in 2011. In order to ensure that this spatial difference is not biasing the averages, we also calculated the average in 2012 for only those stations which were also sampled in 2011. That average is also 38 ± 3 mmol O_2 m^{-2} d^{-1} and thus is still significantly larger than the 2011 average GOP.

Within 2011, GOP is higher on the northern and western edges of the sampling grid; the average GOP along the northern and western edges of the sampling grid being 27 ± 1 mmol O_2 m^{-2} d^{-1} whereas the open basin average GOP = 8 ± 2 mmol O_2 m^{-2} d^{-1}.

There is no statistically significant difference between average NCP in 2011 and in 2012. The average NCP in the basin in 2012, i.e. again excluding shelf stations, is 3.1 ± 0.2 mmol O_2 m^{-2} d^{-1}, whereas the average NCP in the basin in 2011 is 3.2 ± 0.2 mmol O_2 m^{-2} d^{-1}. Again the uncertainty listed is the standard error of the rates within the basin. The typical uncertainty on any given NCP determination is approximately 20% and is set by the uncertainty in air–sea gas exchange since the error in the O_2/Ar measurements offers only a negligible contribution to error in calculated NCP.

In both 2011 and 2012 GOP was more variable than NCP. The coefficient of variation (standard deviation divided by the mean) is 0.7 for GOP but only 0.4 for NCP in 2011. It is 0.7 for GOP and 0.5 for NCP in 2012. The average ratio of NCP/GOP is significantly higher in 2011 than in 2012. In 2011, the average basin-wide NCP/GOP = 0.23 ± 0.02. In 2012, the average basin-wide NCP/GOP = 0.09 ± 0.01.

Rates of productivity on the shelf stations are more variable than the basin stations. Additionally, there are fewer shelf stations than basin ones, inflating the standard error. The 2011 shelf station averages for GOP, NCP and NCP/GOP are 40 ± 12 mmol O_2 m^{-2} d^{-1}, 17 ± 14 mmol O_2 m^{-2} d^{-1}, and 0.25 ± 0.1, respectively. The 2012 averages of the shelf stations, i.e. including both transects, is higher for GOP and similar for NCP, being 81 ± 21 mmol O_2 m^{-2} d^{-1} for GOP, 22 ± 6 mmol O_2 m^{-2} d^{-1} for NCP, and 0.2 ± 0.04 for NCP/GOP. In a comparison of only the shelf along 140°W in both years, the 2011 numbers are much greater than the 2012 ones. The 2012 average of shelf stations along 140°W only is GOP = 17 ± 2 mmol O_2 m^{-2} d^{-1}, NCP = 1.3 ± 0.2 mmol O_2 m^{-2} d^{-1}, and NCP/GOP = 0.07 ± 0.02.

Profiles of $^{17}\Delta$ depths of 600 m were measured 8 times in 2011 and 7 times in 2012. Profiles to depths of 3500 m were measured once in 2011 and twice in 2012 (Fig. 5). These profiles yield interesting qualitative information on $^{17}\Delta$. $^{17}\Delta$ is at a maximum at approximately 50 to 150 m (see inset in Fig. 5 for detail in upper 200 m). This deep subsurface maximum of $^{17}\Delta$ has been observed in the Atlantic and Pacific as well (Ho et al., 2004; Luz and Barkan, 2009; Quay et al., 2010; Stanley et al., 2010) and has often been hypothesized to be a reflection of small amounts of photosynthesis occurring at depths (Nicholson et al., 2014). Since there is relatively little O_2 at such depths, the addition of only a small amount of photosynthetic O_2 is enough to make a large change in the $^{17}\Delta$ signature. Alternatively, it could be a reflection of higher production that occurred in the Pacific-origin water when it was still within the euphotic zone over the northern Bering and Chukchi shelves. $^{17}\Delta$ then decreases until a depth of approximately 500 m. This is either a reflection of Atlantic source water or more likely that the increased age of this water has meant that more $^{17}\Delta$ has been eroded away due to mixing than in the shallower waters. Below approximately 500 m, $^{17}\Delta$ is roughly constant, within measurement uncertainty, at 30 to 40 per meg. This is the same deep value that has been observed in the other ocean basins (Luz and Barkan, 2009) and may likely reflect the long term balance between production when water was at the surface, lateral transport, and vertical mixing.

4. Discussion

4.1. Comparison of 2011 and 2012

The summer of 2012 had record low sea ice extent (National Snow and Ice Data Center, 2012). In contrast, the summer of 2011 had greater sea ice cover. This was true of the entire Arctic, as reported by the NSIDC as well as in the Beaufort Gyre region. For example, in the sea ice

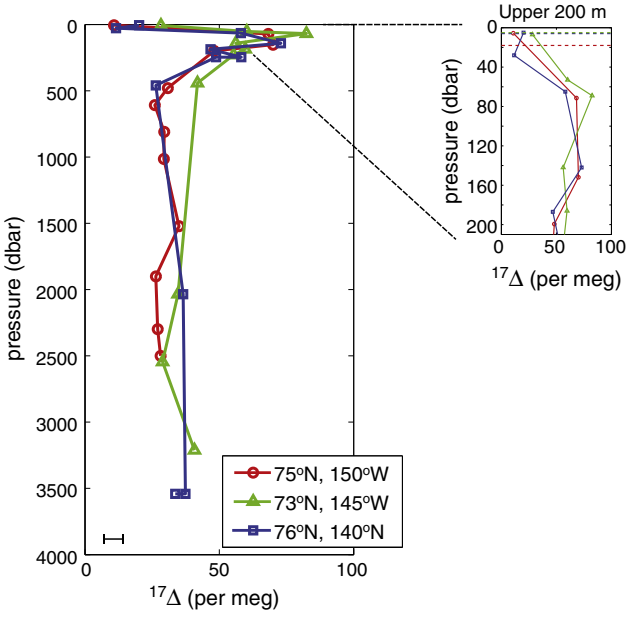

Fig. 5. Water column profiles of $^{17}\Delta$ as a function of depth for one station in 2012 (75°N, 150°W, sampled on Aug 11 2012, red) and two stations in 2011 (73°N, 145°W, sampled on Jul 27 2011, green and 76°N, 140°W, sampled on Aug 9 2011, blue). Measurement uncertainty on the $^{17}\Delta$ is shown by the size of the horizontal line in the lower left corner of the plot. The deep subsurface maximum in $^{17}\Delta$, located between 50 and 150 m, has been observed in other ocean basins and may be a reflection of small amounts of photosynthesis occurring at depth. The inset shows, in detail, the upper 200 m of the profiles, with the mixed layer depth for each station demarcated as a dashed line, same color as the station.

coverage plots in Figs. 2a and 3a, it is clear that 2012 had much less sea ice than in 2011.

GOP was significantly higher in 2012 than in 2011. A histogram of GOP measurements within the basin (Fig. 6) shows that in 2012, GOP was greater than 50 mmol O_2 m^{-2} d^{-1} at 20% of the stations, whereas in 2011, GOP was never greater than 50 mmol O_2 m^{-2} d^{-1}. Furthermore, GOP was below 10 mmol O_2 m^{-2} d^{-1} at 55% of the stations in 2011 but in only 10% of the stations in 2012. The mode of GOP in 2011 was 10 mmol O_2 m^{-2} d^{-1} whereas the mode of GOP in 2012 was 30 mmol O_2 m^{-2} d^{-1}. In 2011, there is likely a bias in the calculated GOP due to the unknown reduction of air–sea gas exchange rate due to the presence of sea ice (Else et al., 2013; Loose et al., 2011). Thus, the 2011 rates reported are upper bounds for GOP and yet they still are significantly smaller than the 2012 rates. Hence our conclusion of greater GOP in 2012 is robust. Notably all the rates reported are for the surface ocean only.

Why is GOP greater in 2012 than in 2011? A likely explanation for the increase in GOP is that the more extensive open water due to the lack of sea ice has resulted in increased photosynthesis by relief of light limitation. An increase in gross primary production corresponding to years of low sea ice has been observed previously in the Amundsen Gulf, which is adjacent to the Canada Basin (Forest et al., 2011) and the Chukchi Sea (Kirchman et al., 2009a) as well as predicted in some numerical simulations of the Arctic (Slagstad et al., 2011). However, other simulations, such as one of the European Corridor, have suggested that changes in sea ice cover will not change gross primary production appreciably (Reigstad et al., 2011; Wassmann et al., 2010). This discrepancy may be due to the differences in physical and biogeochemical conditions between the Western Arctic and the European Corridor. Nonetheless, even in the Canada Basin, the expected direction change of production with melting ice is disputed. For example, in the Canada Basin in particular it has also been suggested that productivity is controlled by nutrients, and not light, and thus that decreased sea ice coverage might not increase primary production (McLaughlin and Carmack, 2010). Surface nitrate and ammonium concentrations in 2011 and 2012 were largely undetectable and there is no reason, a priori, to expect that much lower sea ice coverage would lead to significantly increased nutrients. Hence our data support the hypothesis that lower sea coverage results in an increase in GOP and thus by extension, primary productivity is controlled in at least some part by light. However, our data is only for the surface so a different story might emerge at depth. Sea surface temperature in both years was similar and thus the difference in 2011 vs. 2012 is likely not a result of changes in temperature affecting GOP.

Another possibility, however, is that the difference in the two years is a result of the timing of the cruise in reference to the spring/summer blooms. To the best of our knowledge, no other in situ rates of primary productivity exist in the Canada Basin in the summer of 2011 or 2012. Thus, we examined time-evolving records of primary production, as determined by a satellite-derived algorithm tuned specifically for the Arctic (Arrigo and van Dijken, 2011; Pabi et al., 2008) to determine how the cruise timing aligned with the seasonal bloom. In both 2011 and 2012, the cruise occurred well after the bloom, suggesting that the difference in the years is not related to samples from one year being taken in bloom conditions and the other year samples being collected in post-bloom conditions. While other variables could indeed be different between the years, this study strongly suggests that the lack of sea ice leads to increased gross primary production, even in an intensely stratified system with a deep nitracline and subsurface chlorophyll maximum (McLaughlin and Carmack, 2010). However, given that this study is an observation of a natural system rather than a controlled experiment, we cannot say with certainty that our hypothesis that the difference in productivity between the two years is due to the difference in sea ice cover is correct.

Although GOP was significantly higher in 2012 than in 2011, a histogram of NCP shows that the NCP distribution was similar each year (Fig. 6). NCP is the productivity parameter that is most important for the carbon cycle since it is a measure of the strength of the biological pump and thus of how much CO_2 can be taken-up by biology. The fact that NCP does not change in the two years, and thus perhaps does not change in response to ice cover, suggests that the net biological carbon cycle may not be dependent on sea ice. As the Arctic becomes more ice-free, the net carbon balance may not change.

How can NCP not change and yet GOP change? In order for NCP to be similar and GOP to differ, respiration must be tightly coupled to photosynthesis. Quantitatively, this is shown by a decrease in the NCP/GOP ratio in 2012. The system has become more efficient at internally recycling carbon. Such increased efficiency is reasonable — the NCP/GOP ratios observed in 2011 are on the high end of those typically found in non-bloom conditions (Juranek and Quay, 2013), suggesting

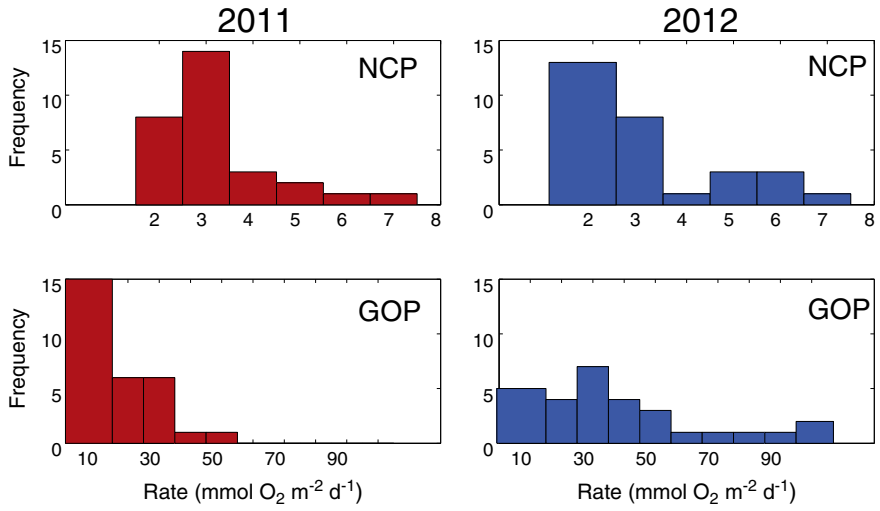

Fig. 6. Histograms of measurements of (a & b) net community production (NCP) in 2011 and 2012 and (c & d) gross oxygen production (GOP) in 2011 and 2012. Note that the distribution of NCP is similar each year. In contrast, the distribution of GOP rates is shifted higher and rates of GOP are significantly larger in 2012 than in 2011. Rates in 2011 were calculated from O_2/Ar and triple oxygen isotope gas tracer data collected in late July and August, 2011 in the Beaufort Gyre region of the Canada Basin (70°N to 80°N, 160°W to 130°W). Rates in 2012 were calculated from O_2/Ar and triple oxygen isotope gas tracer data collected in August and early September, 2012 in the same region. See Figs. 1–3 for exact sample locations.

that there is certainly "room" for the system to become more efficient. The NCP/GOP ratios observed in 2012 are more typical of oligotrophic systems worldwide (Juranek and Quay, 2013).

NCP is defined as photosynthesis minus autotrophic and heterotrophic respiration and we do not know if the increase in respiration is due to the autotrophic component or the heterotrophic one or both. If heterotrophic, it could be either due to changes in bacterial production rates or zooplankton grazing rates. It has been estimated that bacterial production and zooplankton respiration account for approximately equal proportions of respiration in the Canada Basin (Tremblay et al., 2012). Bacterial abundance was measured in 2011 and in 2012 and did not show statistically significant differences between the two years (B. Li, personal communication). Micro- and meso-zooplankton data is not available for both years.

The hypothesis engendered by this work is depicted in cartoon fashion in Fig. 7. We hypothesize that the lack of sea ice in 2012 leads to more light penetration and thus increased rates of photosynthesis in 2012. *Micromonas*, the dominant picoplankton in the Beaufort Gyre (Balzano et al., 2012; Lovejoy and Potvin, 2011; Lovejoy et al., 2007), has been shown to be more responsive to increased light than to increased nutrients (Terrado et al., 2008). We further hypothesize that the grazing community, most likely microzooplankton including small flagellate phagotrophic protists (Monier et al., 2013), increase in response to the increased phytoplankton. Thus there is no net change in community production although an increase in gross oxygen production is observed.

4.2. Shelf-to-basin transitions

It is well known that the shelves in the Arctic Ocean are much more productive than the basins (e.g. Carmack et al., 2006). In this study, we examined the gradients of NCP and GOP between the shelf and basin

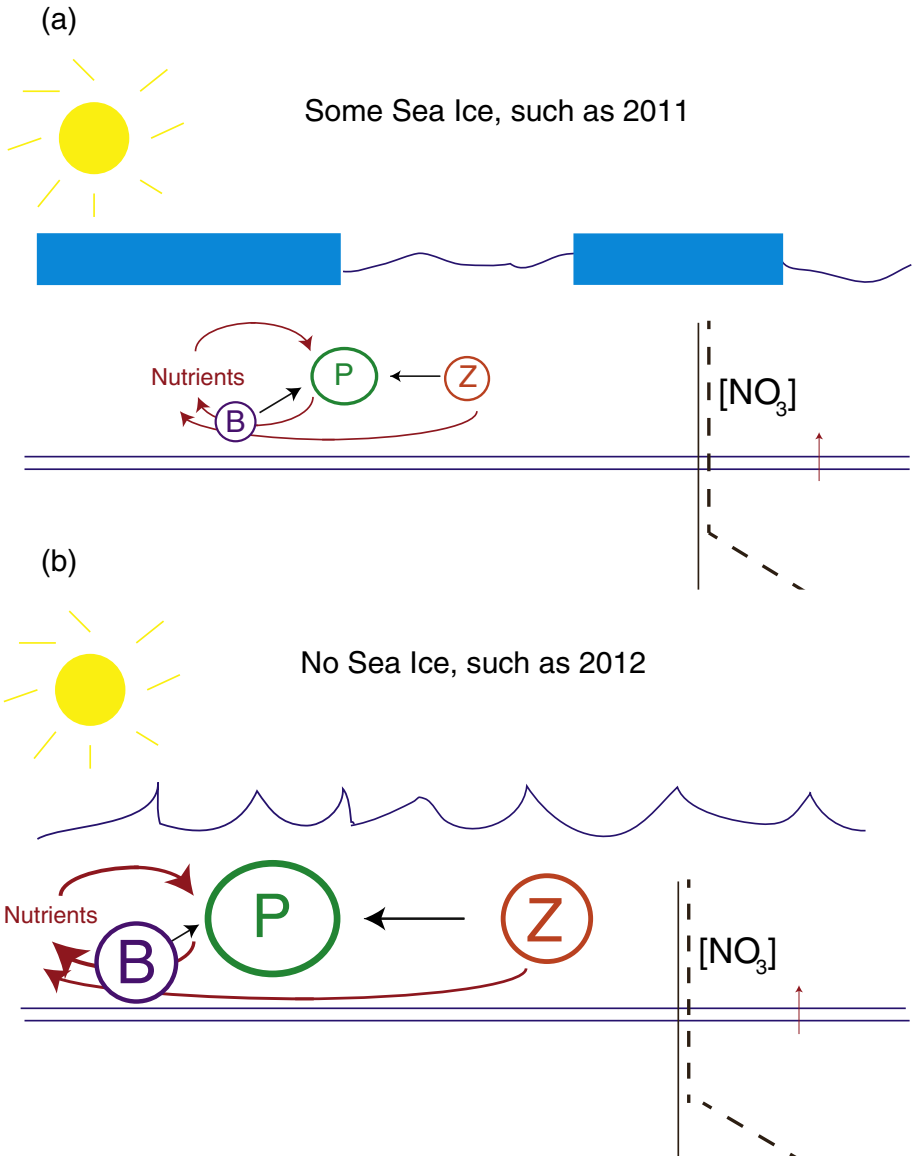

Fig. 7. Cartoon depicting change in biological production as a function of ice cover. (a) In a year with more sea ice, such as 2011, the sea ice (blue rectangle) blocks some of the incoming irradiance. Phytoplankton growth (green circle) is relatively small and is well balanced by a grazing community consisting of bacteria (purple circle) and zooplankton (orange circle). Nutrient cycling (red arrows) is modest. (b) In a year with little or no sea ice, such as 2012, much more light reaches the phytoplankton resulting in a large increase in photosynthetic production. But the grazing community, especially the microzooplankton, is more active as well and thus there is similar net community production in both years. The increase in rates of photosynthesis and respiration is accompanied by increased rates of recycling of nutrients (larger red arrows). Both situations would have almost zero nitrate in the surface water and an increase of nitrate below the nitracline, which is deeper than the mixed layer (black profiles). In both situations, only small vertical fluxes of nitrate from below the nitracline would reach the surface (thin red arrow).

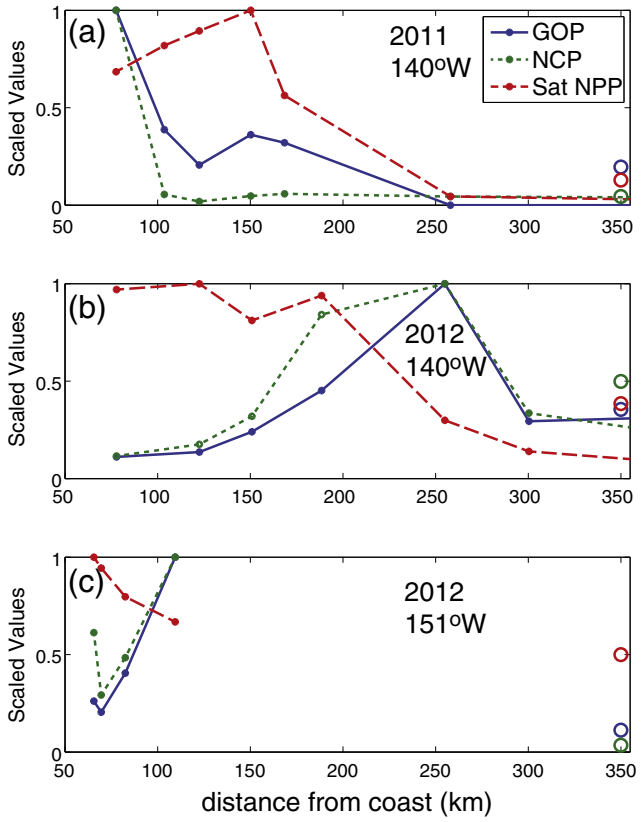

Fig. 8. Shelf to basin gradients along coastal transects along (a) 140°W in 2011 (sampled on July 26, 2011 and Aug 14, 2011), (b) 140°W in 2012 (sampled on Aug 14 and 15, 2012), and (c), 151°W in 2012 (sampled on Aug 9, 2012). In all cases, rates of GOP (blue), NCP (green), and NPP predicted from a satellite algorithm tuned for the Arctic (Arrigo and van Dijken, 2011; Pabi et al., 2008) are normalized to their highest values in the transect. Solid markers denote positions at which rates were calculated from in situ gas tracers. Although the satellite algorithm had estimates everywhere along the transect, it was subsampled at the same locations as the tracer data for better comparability. Open circles at the right edge of the plot depict the basin averaged rates, scaled in the same way as the coastal transect. All variables are plotted as a function of distance from the shore. The shelfbreak (defined as where depth >70 m) occurs at 65 km offshore on the 140°W transect and 59 km offshore on the 151°W transect.

interior. In 2011, stations were measured on one transect from ~75 km offshore to 350 km offshore along 140°W. In 2012, that 140°W transect was reoccupied and stations were also occupied along an additional shorter diagonal transect at 151°W. The transect data is displayed in Figs. 2 to 4 but the values are frequently offscale since the shelf areas are so different than the basin interior. Thus Fig. 8 displays the transect data as a function of distance off-shore. GOP, NCP and satellite-derived NPP are scaled relative to their maximum value on a given transect. This allows clear examination of changes of productivity rates over the length of the transect and also allows easy comparison of the shelf values to the average of interior basin stations (shown as open circles). In 2011, GOP and NCP decrease quickly as one moves off-shore. Interestingly, GOP and NCP are decoupled — GOP decreases more slowly than NCP. This decoupling results in a very high NCP/GOP ratio at the innermost shelf station, i.e. a very efficient export of carbon at that station. Coastal upwelling near shore may be biasing the gas tracer derived estimates of NCP to be too low and GOP to be too high since water below the mixed layer is depleted in O_2/Ar and elevated in $^{17}\Delta$. This is especially true in 2011 and for the 151°W transect in 2012 (see Section 2.2 for discussion of coastal upwelling effects). Thus the trends we see of GOP changing less than NCP may be even more pronounced than shown by these data. The fact that NCP changes more than GOP does suggests that respiration and grazing are more sensitive to the shelf to basin transition than photosynthesis is. This is interesting since a suggested reason for increased productivity on the shelf is increased nutrients due to coastal upwelling (Pickart et al., 2013), which might be expected to benefit phytoplankton more than zooplankton or bacteria. A comparison of gradient in the satellite-derived NPP with the gradient in GOP is discussed in Section 4.5. Chlorophyll decreases along the transects less steeply than NCP or GOP (not shown). Nitrate concentrations are undetectable at all shelf stations and gradients of phosphate and silicate are much smaller than gradients of chlorophyll or productivity.

In 2012, along the same 140°W transect, the highest values of NCP and GOP are no longer immediately adjacent to the shelf, but rather are several hundred km offshore. Additionally, the gradients between shelf to basin, and the absolute magnitudes of the rates, are much smaller in 2012 than in 2011. The maximum GOP on the 140°W shelf in 2012 is only 33 mmol O_2 m^{-2} d^{-1} compared to 338 mmol O_2 m^{-2} d^{-1} in 2011. This difference between the two years is likely a result of timing of the cruise. In 2012, the coastal transect was occupied 20 days later than in 2011. Examination of the satellite-derived NPP for the region shows that in 2011, the coastal stations were occupied in the midst of a shelf bloom, whereas in 2012, the coastal stations were occupied after a bloom had faded.

In 2012, an additional shorter transect on a diagonal around 151°W was sampled. This line was much more productive than the 140°W transect and had much larger gradients of production between shelf and basin. GOP on the shelf was ten times larger than the basin average and NCP was thirty times larger than the basin average. Production is higher 100 km offshore than at the nearest shore station. Similar to in 2011, the gradient in GOP is smaller than the gradient in NCP, again suggesting that the shelf to basin differences matter more for respiration than for photosynthesis. The gradient in chlorophyll (not shown) on the 140°W line also peaks offshore but has a less steep gradient than NCP, GOP or NPP. As in 2011, nitrate concentrations are undetectable at all shelf stations and there is not much of a gradient in phosphate or silicate across the coastal transects.

4.3. Correlations with sea ice coverage within 2011

Above, we describe the effect of sea ice on GOP when comparing the years of 2011 and 2012; but is there an effect of sea ice coverage within 2011, a year where the total ice coverage of stations ranged from 0% to 90%? There is debate in the literature as to whether primary productivity is increased in the region of actively melting ice, i.e. the marginal ice zone, with some studies saying that it is (Arrigo et al., 2012; Slagstad et al., 2011) and others saying that it is not (Wassmann, 2011; Wassmann et al., 2011), although the efficiency of export may be increased in the marginal ice zone (Reigstad et al., 2011). In this study, we cannot unambiguously determine trends for GOP or NCP individually with sea ice due to uncertainties in the effect of sea ice cover on gas exchange (this is not an issue for the 2011 vs. 2012 comparison since any gas exchange effects of sea ice would magnify the differences that we found, rather than diminish them). However, we can compare the ratio of NCP/GOP since gas exchange does not affect that ratio. We find that NCP/GOP is significantly correlated with sea ice coverage in 2011 ($P = 0.001$, $R = -0.49$ for NCP/GOP). In particular, in the region with the highest ice coverage (northern and western edges of the sampling grid), the ratio of NCP/GOP is over two times smaller than in the interior of the basin (20 to 50% ice coverage). These differences are due to changes in GOP rather than in NCP.

All the sea ice observed in 2011 was rotten, with large melt ponds. Recently, high rates of productivity were found under sea ice that had large melt ponds in it (Arrigo et al., 2012) and thus it is likely that photosynthesis is occurring under the ice, resulting in increased GOP. Or potentially, fertilization from the melting ice may be stimulating GOP. In contrast, NCP does not change, resulting in a smaller NCP/GOP. A negative correlation of NCP/GOP with total ice coverage, as well as the relatively low average value of NCP/GOP in the region with almost 90% ice cover, implies that a smaller fraction of carbon is

exported from the surface ocean when the ice is starting to melt. Thus the microbial loop appears to become more efficient in the ice-edge bloom regions. This may be because bacteria are typically limited by carbon and during the ice-edge bloom, this limitation is lifted. A high degree of bacterial–phytoplankton coupling was also observed in the Amundsen Gulf (Forest et al., 2011) but has not been observed in all areas within the Arctic Ocean (Kirchman et al., 2009a, 2009b).

4.4. Correlations of productivity rates with environmental variables

In 2011, we found that GOP had more significant and stronger correlations with environmental variables such as nutrient concentrations, temperature and salinity, and depth of the deep chlorophyll maximum, than NCP with the same variables (Table 1). This suggests that the environmental controls are acting more strongly on rates of photosynthesis than on carbon export. In 2011, positive correlations existed between GOP and PO_4 and between GOP and salinity. Positive correlations also existed between NCP and PO_4 and between NCP and salinity. The Beaufort Gyre has been reported to be nitrogen limited (e.g. Tremblay et al., 2006) and NO_3 concentrations are usually undetectable in the surface water, precluding a correlation with nitrate. However, PO_4 is often delivered to the water in a similar proportion to NO_3, although denitrification on the shelf may change the N/P ratio. We can thus use the observed positive correlation of GOP and NCP with PO_4 as a rough proxy for a correlation with "available NO_3" — the NO_3 that once was available to the community. However, we cannot exclude the possibility that the correlations with PO_4 are a result of the correlation of GOP and NCP with salinity since salinity was well correlated with PO_4. Interestingly, there is no correlation of PO_4 with GOP or NCP in 2012. This is surprising since lack of ice would presumably make light less limiting and thus nutrients more important.

The positive correlations between salinity and NCP and GOP in 2011 may be a result of the effect of sea ice melting. Regions with higher ice coverage have higher salinity since extensive melting has not happened yet. They also have higher rates of biological productivity, as described in Section 4.3. In 2012, there is still a correlation, albeit a weaker one, between GOP and salinity. In this case, all the ice had already melted before the averaging time of the in situ gas tracers but perhaps the salinity signal is a remnant of previous ice cover.

4.5. Comparison to satellite productivity algorithm

We compare primary productivity estimates from a satellite algorithm tuned specifically for the Arctic (Arrigo and van Dijken, 2011; Pabi et al., 2008) to the in situ rates of primary production calculated from the in situ gas tracers. The details of the comparison are described below. In short, the main finding is that the magnitude of the satellite estimates agrees well with the rates calculated from in situ data but the pattern between the years does not. In particular, the satellite algorithm predicts that the 2011 GOP rates are double that of the 2012 GOP rates but we find from gas tracers that the 2012 GOP is greater than 2011.

Table 1
Correlation coefficients (R) for significant correlations ($P < 0.05$) between environmental variables and rates of gross oxygen production (GOP), net community production (NCP), and NCP/GOP in 2011. Insignificant correlations are shown with a "–." Correlation coefficients are not shown for 2012 since the only significant correlation in 2012 was between salinity and GOP with a correlation coefficient of 0.4.

Variable	GOP	NCP	NCP/GOP
Ice coverage	0.55	–	−0.49
PO4	0.44	0.38	−0.33
Temperature	−0.49	–	0.53
Salinity	0.60	0.52	–
Depth of DCM	0.5	−0.45	–

Satellite algorithms for primary productivity give estimates of net primary productivity (NPP) rather than NCP or GOP. We can compare the rates that we calculated in this study to satellite estimates by taking into account that GOP = NPP + autotrophic respiration. If there are no variations in autotrophic respiration, then GOP = c NPP where c is a constant multiplier. While there are likely some variations in autotrophic respiration, both laboratory and field data suggest that c is often nearly constant. In particular, laboratory experiments have shown that c = 3.3 for a diatom grown on nitrate (Halsey et al., 2010). In the field, bottle incubation experiments have shown that c = 2.7 (Marra, 2002). Field estimates comparing triple oxygen isotopic derived GOP to NPP estimates suggest that c ranges 2 to 3 in steady state conditions (Quay et al., 2010) and may be as large as 5 or 6 in actively changing conditions (Luz and Barkan, 2009; Robinson et al., 2009; Stanley et al., 2010). However, these high values of c may be a result of entrainment biasing the triple oxygen isotope GOP numbers (Nicholson et al., 2012). If c is constant, or near constant, we would expect the trends of NPP derived from a satellite algorithm tuned for the Arctic (Arrigo and van Dijken, 2011; Pabi et al., 2008) to be similar to the trends shown by GOP.

NPP determined from the satellite algorithm interpolated to the station locations for the day of collection is shown in Fig. 9. There are not satellite-based estimates for all stations since the presence of either clouds or sea ice precludes a satellite estimate. The satellite algorithm gives NPP in units of mg C m^{-2} d^{-1}. In order to compare the numbers more easily to the GOP estimates presented here, we have converted the units to mmol O_2 m^{-2} d^{-1}, assuming a photosynthetic quotient of 1.2 for a community growing on a mix of recycled and new production (Laws, 1991).

In order to compare NPP in 2011 vs. those in 2012, we calculated the average in all non-shelf stations each year and also the average each year in a subsampled region where estimates were available for both years. Otherwise, there might be a bias since there were more northerly satellite estimates in 2012 than in 2011. The average of non-shelf NPP from the satellite algorithm is 16 ± 1 mmol O_2 m^{-2} d^{-1} in 2011 and 8 ± 0.5 mmol O_2 m^{-2} d^{-1} in 2012. The coefficient of variation for the satellite algorithm estimates is 2.8 in 2011 and 2.6 in 2012. When subsampled, the averages are almost identical: NPP average of 16 ± mmol O_2 m^{-2} d^{-1} in 2011 and 9 ± 0.7 mmol O_2 m^{-2} d^{-1} in 2012. When scaled by a factor of 2.7, the satellite algorithm predicts a "GOP" of 43 ± 3 mmol O_2 m^{-2} d^{-1} in 2011 and 22 ± 2 mmol O_2 m^{-2} d^{-1} in 2012.

Thus in 2011, the satellite estimate is larger than the average of the in situ gas tracer-derived GOP but in 2012, it is smaller. In order to see if the difference in 2011 and 2012 estimated by satellites vs. in situ tracers was related to time of year of the cruise, we calculated the average satellite rates for time period covered by the 2011 cruise, for the time period covered by the 2012 cruise, and for the entire period covered by both cruises. In all cases, the satellite predicted higher NPP and GOP in 2011 than in 2012, just the opposite of what we see from the gas tracer data. In other ocean basins, rates of productivity estimated from satellite algorithms often are lower than rates of productivity estimated from triple oxygen isotopes (Juranek and Quay, 2010, 2013; Reuer et al., 2007; Stanley et al., 2010) though in the North Atlantic, satellite estimates agreed well with rates of productivity from triple oxygen isotopes (Quay et al., 2012).

Like the in situ data, the satellite algorithm predicts higher productivity on the shelf stations than in the basin (Fig. 8). However, the gradient between the basin and coast is much steeper for the satellite rates than for the in situ gas tracer rates. For example, in 2011, there is a factor of 5 difference between GOP measured in situ on the shelf vs. the basin average. However, there is approximately a factor of 20 difference in the satellite algorithm NPP between the shelf and basin stations. This may be because satellite algorithms have biases in coastal waters due to signal contamination by colored dissolved organic matter or because the satellite algorithms may be reflecting productivity gradients present

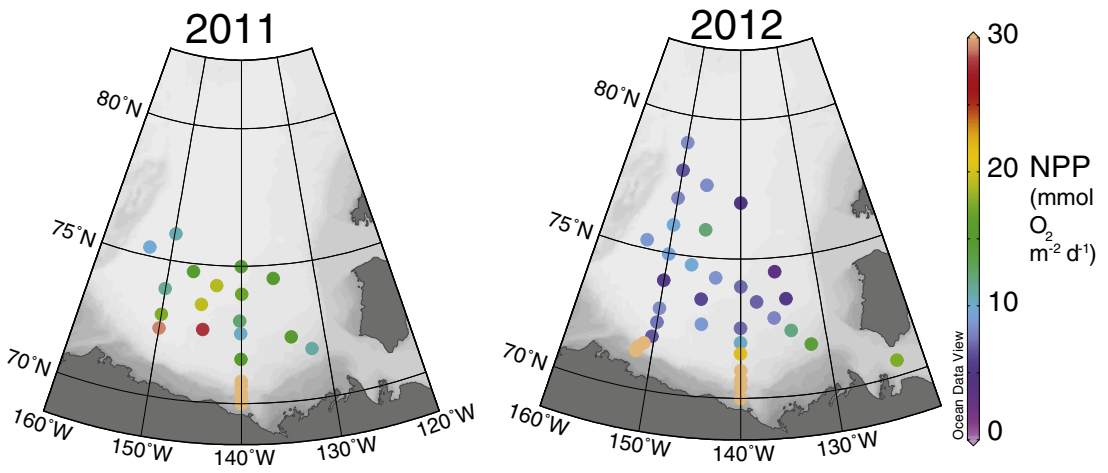

Fig. 9. Rates of net primary production (NPP) as estimated from the satellite algorithm of Pabi et al. (2008) updated by Arrigo and van Dijken (2011) for the Beaufort Gyre region of the Canada Basin for late July and August 2011 and August and early September, 2012. Rates were interpolated from regular gridded maps to the times and locations of the sample points and then converted to units of mmol O_2 m^{-2} d^{-1} using a photosynthetic quotient of 1.2. The values for the coastal transects are off the color scale but can be examined in more detail in Fig. 7.

before the gas tracer data started integrating. A further difference between the satellite algorithm and the in situ rates is that the satellite algorithm predicts in 2011 that the highest rates are 150 m offshore whereas the in situ data predicts the highest GOP closest to the shore station. In 2012, the reverse is true — the satellite algorithm predicts that the highest rates are closest to shore whereas the gas tracer data suggests higher rates offshore.

4.6. Comparison to historical productivity data

Not many measurements of gross primary production exist for the Arctic Ocean, though gross primary production has often been modeled (Reigstad et al., 2011; Slagstad et al., 2011; Wassmann, 2011; Wassmann et al., 2010). Instead, most often NPP is measured using ^{14}C bottle incubations (Marra, 2009). As described in Section 4.5, GOP is likely to equal 2.7 × NPP. Thus, we can compare GOP calculated here to previously determined NPP. When doing so, we find that the values are similar, even though our rates only reflect mixed layer production and thus are likely missing the large subsurface production, estimated to range from 10% to 50% (Arrigo and van Dijken, 2011; Tremblay et al., 2008). NPP are typically reported in units of mg C m^{-2} d^{-1}; an NPP value of 100 mg C m^{-2} d^{-1} is equivalent to a GOP of 27 mmol O_2 m^{-2} d^{-1}. NPP, measured in the Canada Basin in 2002 and 2004 (Kirchman et al., 2009a) was approximately 100 mg C m^{-2} d^{-1} in 2002 and two to three times larger in 2005. The 2002 numbers are very similar to our 2012 rates, especially given the difference in timing of the cruises with respect to blooms, interannual variability, differences in sample location, and differences in depth to which production is integrated. Kirchman et al. (2009a) also examined the differences between shelf, slope and basin and found about a factor of 100 difference in productivity between shelf, slope and basin, which is a larger gradient than we find in this study. In 2007, NPP was measured in the Beaufort Sea on a JOIS expedition. Average NPP within the South Beaufort Sea/Canada Basin was 50 mg C m^{-2} d^{-1} (Tremblay et al., 2012) which is similar to the average GOP that we find in 2011. Carmack et al. (2006) reports rates of total productivity of 30 to 70 g C m^{-2} y^{-1} which if scaled to a 120 day growing season again is in reasonable agreement with the rates we determine, especially since our rates are post-bloom and are only for the mixed layer.

We determined the ratio of NCP/GOP to be on average 0.23 in 2011 and 0.09 in 2012. If one uses the factor of 2.7 to convert GOP to NPP and assumes that NCP equals new production over long enough spatial and temporal scales (Dugdale and Goering, 1967), then the average f-ratio that we determined is 0.62 in 2011 and 0.24 in 2012. This is a large range of f-ratios but is well within the range of f-ratios reported in the literature for the Canada Basin. In the Amundsen Gulf, in 2007, the f-ratio was determined to be 0.64 (Forest et al., 2011). The Amundsen Gulf, however, is more productive than the central Beaufort Sea Basin and thus might be expected to have a higher f-ratio. In 2007, measurements on the JOIS expedition suggested an f-ratio of 0.26 (Tremblay et al., 2012). Carmack et al. (2006) reports that f-ratios can range in the Beaufort shelf from 0.2 to 0.5.

Many fewer estimates of NCP exist than those of f-ratios or NPP. Mathis et al. (2009) quantified NCP using the seasonal drawdown of DIC and nutrients in the Chukchi Sea and also for a few stations in the South Beaufort Sea and Canada Basin. For the Canada Basin, they reported NCP estimates of 8 to 24 mg C m^{-2} d^{-1}, which equals 0.8 to 2.4 mmol O_2 m^{-2} d^{-1}. On the slope/basin interface, Mathis et al. determined NCP to be equal to 45 mg C m^{-2} d^{-1}, corresponding to 4.5 mmol O_2 m^{-2} d^{-1}. This is in good agreement with the NCP that we find in this study, namely an average of 3 mmol O_2 m^{-2} d^{-1} for the basin stations.

Coupled physical and biological models are used to examine trends in rates of biological productivity in the Arctic. A recent study compared five such models (Popova et al., 2012). The rates of GOP determined from in situ tracers in this study are within the range of the scaled NPP estimated by 4 of the 5 models used in the comparison study. Only the Ocean Circulation and Climate Advanced Modeling (OCCAM) project model predicted very different rates than that determined in this study. OCCAM had the longest unconstrained run and the coarsest resolution of the models in Popova et al. (2012) study.

5. Conclusions

In this study, we quantified GOP and NCP from in situ gas tracers in the Beaufort Gyre in 2011 and 2012. The productivity rates we report are for the mixed layer only and integrate over several days. Most notably, we found that GOP was a factor of three greater in the record-low sea ice year of 2012 compared to 2011, a year with more sea ice. However, NCP was the same in the two years. Interestingly, this region of the Canada Basin is expected to be nutrient limited and thus one might predict that a change in sea ice cover would not have a large effect on gross primary production. A satellite-derived primary productivity algorithm tuned for the Arctic (Arrigo and van Dijken, 2011; Pabi et al., 2008) did not capture this interannual difference, instead predicting that NPP at sampled stations would be higher in 2011 than in 2012.

The results presented in this study are only for one month and only for the mixed layer. If the trends we find here hold true in other seasons and locations, they have profound implications for the question of whether primary productivity will increase as the Arctic becomes ice-free. This study suggests that although changing sea ice cover may affect gross primary productivity, it may not change net community productivity. In other words, photosynthesis may increase as sea ice decreases, but net carbon uptake may not change. Thus the question of whether the Arctic will become more productive may depend on whether by productive, only photosynthesis is meant or if net biological uptake is the important consideration.

We found a larger gradient between the shelf stations and basin ones for NCP than GOP in 2011 but a smaller one for NCP than GOP in 2012. For both years, the gradients determined for the in situ GOP estimates were within the range of gradients reported in the literature but smaller than those predicted by the satellite-based primary productivity algorithm.

We examined the relationship between NCP, GOP, and ice cover in 2011 in order to investigate if there was increased production in the marginal ice zone. We found an increase in GOP and a decrease in NCP/GOP ratio in the regions with highest ice cover, rotten ice, and large melt ponds. NCP however was not correlated with ice cover. Once again, NCP was less variable than GOP, suggesting a tightly coupled response of the heterotrophic community to changes in primary production.

Overall, the main conclusion of this paper – that rates of GOP in the ice-free year are larger than rates in the heavier ice year but rates of NCP are similar between the two years – has profound implications on carbon cycling in the Canada Basin. In order to verify these findings, it would be useful to have more in situ gas tracer measurements at varying months within a given year, both in the Canada Basin and in other areas of the Arctic Ocean. At the moment, there is no capability for collecting samples for triple oxygen isotopes on moorings. However, all ships going to the region could potentially collect bottles for analysis, since sample collection is fairly straightforward. Having a long term time-series with many samples distributed throughout the summer – or even throughout the whole year – in several of the Arctic basins would provide key information on how biological productivity and the carbon cycle changes as the Arctic ocean warms. Additionally, a time-series in a given basin would allow quantitative information on rates of biological productivity below the mixed layer.

Acknowledgments

We sincerely thank the scientific teams of Fisheries and Oceans Canada's Joint Ocean Ice Studies expedition and Woods Hole Oceanographic Institution's Beaufort Gyre Observing System. The hydrographic, nutrient, and chlorophyll data were collected and made available by the Beaufort Gyre Exploration Program based at the Woods Hole Oceanographic Institution (http://www.whoi.edu/beaufortgyre) in collaboration with researchers from Fisheries and Oceans Canada at the Institute of Ocean Sciences. We are very grateful to the captains and crews of the Canadian icebreaker *CCGS Louis S. St-Laurent*. Without their hard work, this research would not have been possible. We would like to thank Sarah Zimmerman and Mike Dempsey for the sample collection, Jenny Hutchings and Alice Orlich for the ice observations, Bill Li for the bacterial abundance data, and R. John Nelson for the zooplankton data. We are very grateful to Kevin Arrigo and Gert Van Dijken for making available to us the primary productivity rates estimated from their satellite-based algorithm. This manuscript has been improved thanks to the suggestions of guest editor Alberto Borges and the two anonymous reviewers. We are grateful for Ocean Data View (*Schlitzer, R., Ocean Data View*, http://odv.awi.de, 2013) which was used to make many of the figures in this paper. We thank our funding sources: the National Science Foundation (PLR 1304406, PLR-0856531) and the support of Fisheries and Oceans Canada.

References

Aagaard, K., Carmack, E.C., 1989. The role of sea ice and other fresh-water in the Arctic circulation. J. Geophys. Res.-Oceans 94, 14485–14498. http://dx.doi.org/10.1029/JC094iC10p14485.

Arrigo, K.R., van Dijken, G.L., 2011. Secular trends in Arctic Ocean net primary production. J. Geophys. Res.-Oceans 116 (doi: C0901110.1029/2011jc007151).

Arrigo, K.R., van Dijken, G., Pabi, S., 2008a. Impact of a shrinking Arctic ice cover on marine primary production. Geophys. Res. Lett. 35.

Arrigo, K.R., van Dijken, G.L., Bushinsky, S., 2008b. Primary production in the Southern Ocean, 1997–2006. J. Geophys. Res.-Oceans 113.

Arrigo, K.R., Perovich, D.K., Pickart, R.S., Brown, Z.W., van Dijken, G.L., Lowry, K.E., Mills, M.M., Palmer, M.A., Balch, W.M., Bahr, F., Bates, N.R., Benitez-Nelson, C., Bowler, B., Brownlee, E., Ehn, J.K., Frey, K.E., Garley, R., Laney, S.R., Lubelczyk, L., Mathis, J., Matsuoka, A., Mitchell, B.G., Moore, G.W.K., Ortega-Retuerta, E., Pal, S., Polashenski, C.M., Reynolds, R.A., Schieber, B., Sosik, H.M., Stephens, M., Swift, J.H., 2012. Massive phytoplankton blooms under Arctic sea ice. Science 336, 1408–1408. http://dx.doi.org/10.1126/science.1215065.

Balzano, S., Marie, D., Gourvil, P., Vaulot, D., 2012. Composition of the summer photosynthetic pico and nanoplankton communities in the Beaufort Sea assessed by T-RFLP and sequences of the 18S rRNA gene from flow cytometry sorted samples. ISME J. 6, 1480–1498. http://dx.doi.org/10.1038/ismej.2011.213.

Barkan, E., Luz, B., 2003. High-precision measurements of $^{17}O/^{16}O$ and $^{18}O/^{16}O$ of O_2 and O_2/Ar ratio in air. Rapid Commun. Mass Spectrom. 17, 2809–2814.

Bates, N.R., Mathis, J.T., 2009. The Arctic Ocean marine carbon cycle: evaluation of air–sea CO_2 exchanges, ocean acidification impacts and potential feedbacks. Biogeosciences 6, 2433–2459.

Bates, N.R., Mathis, J.T., Cooper, L.W., 2009. Ocean acidification and biologically induced seasonality of carbonate mineral saturation states in the western Arctic Ocean. J. Geophys. Res.-Oceans 114 (doi: C1100710.1029/2008jc004862).

Bates, N.R., Cai, W.J., Mathis, J.T., 2011. The ocean carbon cycle in the western Arctic Ocean: distributions and air–sea fluxes of carbon dioxide. Oceanography 24, 186–201.

Bender, M., Orchardo, J., Dickson, M.L., Barber, R., Lindley, S., 1999. In vitro O_2 fluxes compared with ^{14}C production and other rate terms during the JGOFS Equatorial Pacific experiment. Deep-Sea Res. Part I-Oceanogr. Res. Pap. 46, 637–654.

Benson, B.B., Krause, D., 1984. The concentration and isotopic fractionation of oxygen dissolved in fresh-water and seawater in equilibrium with the atmosphere. Limnol. Oceanogr. 29, 620–632.

Brown, Z.W., Arrigo, K.R., 2012. Contrasting trends in sea ice and primary production in the Bering Sea and Arctic Ocean. ICES J. Mar. Sci. 69, 1180–1193. http://dx.doi.org/10.1093/icesjms/fss113.

Cai, W.J., Chen, L.Q., Chen, B.S., Gao, Z.Y., Lee, S.H., Chen, J.F., Pierrot, D., Sullivan, K., Wang, Y.C., Hu, X.P., Huang, W.J., Zhang, Y.H., Xu, S.Q., Murata, A., Grebmeier, J.M., Jones, E.P., Zhang, H.S., 2010. Decrease in the CO_2 uptake capacity in an ice-free Arctic Ocean basin. Science 329, 556–559. http://dx.doi.org/10.1126/science.1189338.

Carmack, E., Chapman, D.C., 2003. Wind-driven shelf/basin exchange on an Arctic shelf: the joint roles of ice cover extent and shelf-break bathymetry. Geophys. Res. Lett. 30 (doi: 177810.1029/2003gl017526).

Carmack, E., Barber, D., Christensen, J., Macdonald, R., Rudels, B., Sakshaug, E., 2006. Climate variability and physical forcing of the food webs and the carbon budget on panarctic shelves. Prog. Oceanogr. 71, 145–181. http://dx.doi.org/10.1016/j.pocean.2006.10.005.

Center, N.S.a.I.D., 2012. Arctic sea ice shatters previous low records. http://nsidc.org/news/press/20121002_MinimumPR.html.

Cottrell, M.T., Malmstrom, R.R., Hill, V., Parker, A.E., Kirchman, D.L., 2006. The metabolic balance between autotrophy and heterotrophy in the western Arctic Ocean. Deep-Sea Res. Part I-Oceanogr. Res. Pap. 53, 1831–1844. http://dx.doi.org/10.1016/j.dsr.2006.08.010.

Craig, H., Hayward, T., 1987. Oxygen supersaturation in the ocean: biological versus physical contributions. Science 235, 199–202.

Dugdale, R.C., Goering, J.J., 1967. Uptake of new and regenerated forms of nitrogen in primary productivity. Limnol. Oceanogr. 12, 196–206.

Eisenstadt, D., Barkan, E., Luz, B., Kaplan, A., 2010. Enrichment of oxygen heavy isotopes during photosynthesis in phytoplankton. Photosynth. Res. 103, 97–103. http://dx.doi.org/10.1007/s11120-009-9518-z.

Else, B.G.T., Papakyriakou, T.N., Asplin, M.G., Barber, D.G., Galley, R.J., Miller, L.A., Mucci, A., 2013. Annual cycle of air–sea CO_2 exchange in an Arctic Polynya Region. Glob. Biogeochem. Cycles 27, 388–398. http://dx.doi.org/10.1002/gbc.20016.

Emerson, S., Quay, P., Stump, C., Wilbur, D., Knox, M., 1991. O_2, Ar, N_2, and ^{222}Rn in surface waters of the subarctic ocean: Net biological O_2 production. Glob. Biogeochem. Cycles 5, 49–69.

Emerson, S., Quay, P., Wheeler, P.A., 1993. Biological productivity determined from oxygen mass-balance and incubation experiments. Deep-Sea Res. Part I-Oceanogr. Res. Pap. 40, 2351–2358.

Emerson, S., Quay, P.D., Stump, C., Wilbur, D., Schudlich, R., 1995. Chemical tracers of productivity and respiration in the subtropical Pacific-Ocean. J. Geophys. Res.-Oceans 100, 15873–15887.

Emerson, S., Stump, C., Wilbur, D., Quay, P., 1999. Accurate measurement of O_2, N_2, and Ar gases in water and the solubility of N_2. Mar. Chem. 64, 337–347.

Falkowski, P.G., Oliver, M.J., 2007. Mix and match: how climate selects phytoplankton. Nat. Rev. Microbiol. 5, 813–819. http://dx.doi.org/10.1038/nrmicro1751.

Fanning, K.A., Torres, L.M., 1991. ^{222}Rn and ^{226}Ra — indicators of sea-ice effects on air–sea gas-exchange. Polar Res. 10, 51–58.

Forest, A., Tremblay, J.E., Gratton, Y., Martin, J., Gagnon, J., Darnis, G., Sampei, M., Fortier, L., Ardyna, M., Gosselin, M., Hattori, H., Nguyen, D., Maranger, R., Vaque, D., Marrase, C., Pedros-Alio, C., Sallon, A., Michel, C., Kellogg, C., Deming, J., Shadwick, E., Thomas, H.,

Link, H., Archambault, P., Piepenburg, D., 2011. Biogenic carbon flows through the planktonic food web of the Amundsen Gulf (Arctic Ocean): a synthesis of field measurements and inverse modeling analyses. Prog. Oceanogr. 91, 410–436. http://dx.doi.org/10.1016/j.pocean.2011.05.002.

Fransson, A., Chierici, M., Nojiri, Y., 2009. New insights into the spatial variability of the surface water carbon dioxide in varying sea ice conditions in the Arctic Ocean. Cont. Shelf Res. 29, 1317–1328. http://dx.doi.org/10.1016/j.csr.2009.03.008.

Frey, K.E., Smith, L.C., 2005. Amplified carbon release from vast West Siberian peatlands by 2100. Geophys. Res. Lett. 32 (doi: L0940110.1029/2004gl022025).

Grebmeier, J.M., Moore, S.E., Overland, J.E., Frey, K.E., Gradinger, R., 2010. Biological response to recent Pacific Arctic sea ice retreats. Eos Transactions AGU 91, 161–162.

Guo, L.D., Macdonald, R.W., 2006. Source and transport of terrigenous organic matter in the upper Yukon River: evidence from isotope ($\delta^{13}C$, $\Delta^{14}C$, and $\delta^{15}N$) composition of dissolved, colloidal, and particulate phases. Glob. Biogeochem. Cycles 20 (doi: Gb2011 10.1029/2005gb002593).

Halsey, K.H., Milligan, A.J., Behrenfeld, M.J., 2010. Physiological optimization underlies growth rate-independent chlorophyll-specific gross and net primary production. Photosynth. Res. 103, 125–137. http://dx.doi.org/10.1007/s11120-009-9526-z.

Hamme, R.C., Cassar, N., Lance, V.P., Vaillancourt, R.D., Bender, M.L., Strutton, P.G., Moore, T.S., DeGrandpre, M.D., Sabine, C.L., Ho, D.T., Hargreaves, B.R., 2012. Dissolved O_2/Ar and other methods reveal rapid changes in productivity during a Lagrangian experiment in the Southern Ocean. J. Geophys. Res.-Oceans 117, C00F12. http://dx.doi.org/10.1029/2011JC007046.

Helman, Y., Barkan, E., Eisenstadt, D., Luz, B., Kaplan, A., 2005. Fractionation of the three stable oxygen isotopes by oxygen-producing and oxygen-consuming reactions in photosynthetic organisms. Plant Physiol. 138, 2292–2298. http://dx.doi.org/10.1104/pp. 105.063768.

Hendricks, M.B., Bender, M.L., Barnett, B.A., 2004. Net and gross O_2 production in the Southern Ocean from measurements of biological O_2 saturation and its triple isotope composition. Deep-Sea Res. Part I-Oceanogr. Res. Pap. 51, 1541–1561.

Hendricks, M.B., Bender, M.L., Barnett, B.A., Strutton, P., Chavez, F.P., 2005. Triple oxygen isotope composition of dissolved O_2 in the equatorial Pacific: a tracer of mixing, production, and respiration. J. Geophys. Res.-Oceans 110. http://dx.doi.org/10.1029/2004JC002735.

Hill, V., Cota, G., 2005. Spatial patterns of primary production on the shelf, slope and basin of the Western Arctic in 2002. Deep-Sea Res. II 52, 3344–3354. http://dx.doi.org/10.1016/j.dsr2.2005.10.001.

Ho, D.T., Zappa, C.J., McGillis, W.R., Bliven, L.F., Ward, B., Dacey, J.W.H., Schlosser, P., Hendricks, M.B., 2004. Influence of rain on air–sea gas exchange: lessons from a model ocean. J. Geophys. Res.-Oceans 109. http://dx.doi.org/10.1029/2003JC001806.

Holding, J.M., Duarte, C.M., Arrieta, J.M., Vaquer-Sunyer, R., Coello-Camba, A., Wassmann, P., Agusti, S., 2013. Experimentally determined temperature thresholds for Arctic plankton community metabolism. Biogeosciences 10, 357–370. http://dx.doi.org/10.5194/bg-10-357-2013.

Jonsson, B.F., Doney, S.C., Dunne, J., Bender, M., 2013. Evaluation of the Southern Ocean O_2/Ar-based NCP estimates in a model framework. J. Geophys. Res. Biogeosci. 118, 385–399.

Juranek, L.W., Quay, P.D., 2005. In vitro and in situ gross primary and net community production in the North Pacific Subtropical Gyre using labeled and natural abundance isotopes of dissolved O_2. Glob. Biogeochem. Cycles 19. http://dx.doi.org/10.1029/2004GB002384.

Juranek, L.W., Quay, P.D., 2010. Basin-wide photosynthetic production rates in the subtropical and tropical Pacific Ocean determined from dissolved oxygen isotope ratio measurements. Glob. Biogeochem. Cycles 24. http://dx.doi.org/10.1029/2009GB003492.

Juranek, L.W., Quay, P.D., 2013. Using triple isotopes of dissolved oxygen to evaluate global marine productivity. In: Carlson, C.A., Giovannoni, S.J. (Eds.), Annual Review of Marine Science. Annual Reviews, Palo Alto, vol. 5, pp. 503–524.

Juranek, L.W., Quay, P.D., Feely, R.A., Lockwood, D., Karl, D.M., Church, M.J., 2012. Biological production in the NE Pacific and its influence on air–sea CO_2 flux: evidence from dissolved oxygen isotopes and O_2/Ar. J. Geophys. Res.-Oceans. http://dx.doi.org/10.1029/2011JC007450.

Kalnay, E., Kanamitsu, M., Kistler, R., Collins, W., Deaven, D., Gandin, L., Iredell, M., Saha, S., White, G., Woollen, J., Zhu, Y., Chelliah, M., Ebisuzaki, W., Higgins, W., Janowiak, J., Mo, K.C., Ropelewski, C., Wang, J., Leetmaa, A., Reynolds, R., Jenne, R., Joseph, D., 1996. The NCEP/NCAR 40-year reanalysis project. Bull. Am. Meteorol. Soc. 77, 437–471.

Kirchman, D.L., Hill, V., Cottrell, M.T., Gradinger, R., Malmstrom, R.R., Parker, A., 2009a. Standing stocks, production, and respiration of phytoplankton and heterotrophic bacteria in the western Arctic Ocean. Deep-Sea Res. II 56, 1237–1248. http://dx.doi.org/10.1016/j.dsr2.2008.10.018.

Kirchman, D.L., Moran, X.A.G., Ducklow, H., 2009b. Microbial growth in the polar oceans — role of temperature and potential impact of climate change. Nat. Rev. Microbiol. 7, 451–459. http://dx.doi.org/10.1038/nrmicro2115.

Kistler, R., Kalnay, E., Collins, W., Saha, S., White, G., Woollen, J., Chelliah, M., Ebisuzaki, W., Kanamitsu, M., Kousky, V., van den Dool, H., Jenne, R., Fiorino, M., 2001. The NCEP-NCAR 50-year reanalysis: monthly means CD-ROM and documentation. Bull. Am. Meteorol. Soc. 82, 247–267.

Kritzberg, E.S., Duarte, C.M., Wassmann, P., 2010. Changes in Arctic marine bacterial carbon metabolism in response to increasing temperature. Polar Biol. 33, 1673–1682. http://dx.doi.org/10.1007/s00300-010-0799-7.

Kwok, R., Cunningham, G.F., Wensnahan, M., Rigor, I., Zwally, H.J., Yi, D., 2009. Thinning and volume loss of the Arctic Ocean sea ice cover: 2003–2008. J. Geophys. Res.-Oceans 114 (doi: C0700510.1029/2009jc005312).

Lammerzahl, P., Rockmann, T., Brenninkmeijer, C.A.M., Krankowsky, D., Mauersberger, K., 2002. Oxygen isotope composition of stratospheric carbon dioxide. Geophys. Res. Lett. 29. http://dx.doi.org/10.1029/2001GL014343.

Lavoie, D., Denman, K.L., Macdonald, R.W., 2010. Effects of future climate change on primary productivity and export fluxes in the Beaufort Sea. J. Geophys. Res.-Oceans 115 (doi: C0401810.1029/2009jc005493).

Laws, E.A., 1991. Photosynthetic quotients, new production and net community production in the open ocean. Deep-Sea Res. Part a-Oceanographic Res. Pap. 38, 143–167.

Laws, E.A., Landry, M.R., Barber, R.T., Campbell, L., Dickson, M.L., Marra, J., 2000. Carbon cycling in primary production bottle incubations: inferences from grazing experiments and photosynthetic studies using ^{14}C and ^{18}O in the Arabian Sea. Deep-Sea Res. II 47, 1339–1352.

Li, W.K.W., McLaughlin, F.A., Lovejoy, C., Carmack, E.C., 2009. Smallest algae thrive as the Arctic Ocean freshens. Science 326, 539–539. http://dx.doi.org/10.1126/science.1179798.

Loose, B., McGillis, W.R., Schlosser, P., Perovich, D., Takahashi, T., 2009. Effects of freezing, growth, and ice cover on gas transport processes in laboratory seawater experiments. Geophys. Res. Lett. 36. http://dx.doi.org/10.1029/2008GL036318.

Loose, B., Schlosser, P., Perovich, D., Ringelberg, D., Ho, D.T., Takahashi, T., Richter-Menge, J., Reynolds, C.M., McGillis, W.R., Tison, J.L., 2011. Gas diffusion through columnar laboratory sea ice: implications for mixed-layer ventilation of CO_2 in the seasonal ice zone. Tellus Ser. B Chem. Phys. Meteorol. 63 (1), 23–39.

Lott, D.E., 2001. Improvements in noble gas separation methodology: a nude cryogenic trap. Geochem. Geophys. Geosyst. 2. http://dx.doi.org/10.129/2001GC000202.

Lovejoy, C., Potvin, M., 2011. Microbial eukaryotic distribution in a dynamic Beaufort Sea and the Arctic Ocean. J. Plankton Res. 33, 431–444. http://dx.doi.org/10.1093/plankt/fbq124.

Lovejoy, C., Vincent, W.F., Bonilla, S., Roy, S., Martineau, M.J., Terrado, R., Potvin, M., Massana, R., Pedros-Alio, C., 2007. Distribution, phylogeny, and growth of cold-adapted picoprasinophytes in arctic seas. J. Phycol. 43, 78–89. http://dx.doi.org/10.1111/j.1529-8817.2006.00310.x.

Luz, B., Barkan, E., 2000. Assessment of oceanic productivity with the triple-isotope composition of dissolved oxygen. Science 288, 2028–2031.

Luz, B., Barkan, E., 2009. Net and gross oxygen production from O_2/Ar, $^{17}O/^{16}O$ and $^{18}O/^{16}O$ ratios. Aquat. Microb. Ecol. 56, 133–145.

Luz, B., Barkan, E., 2011. Proper estimation of marine gross O_2 production with $^{17}O/^{16}O$ and $^{18}O/^{16}O$ ratios of dissolved O_2. Geophys. Res. Lett. 38 (doi: L1960610.1029/2011gl049138).

Luz, B., Barkan, E., Bender, M.L., Thiemens, M.H., Boering, K.A., 1999. Triple-isotope composition of atmospheric oxygen as a tracer of biosphere productivity. Nature 400, 547–550.

Markus, T., Stroeve, J.C., Miller, J., 2009. Recent changes in Arctic sea ice melt onset, freezeup, and melt season length. J. Geophys. Res.-Oceans 114.

Marra, J., 2002. Approaches to the Measurement of Plankton Production. Blackwell, Malden, MA.

Marra, J., 2009. Net and gross productivity: weighing in with ^{14}C. Aquat. Microb. Ecol. 56, 123–131.

Maslanik, J., Stroeve, J., Fowler, C., Emery, W., 2011. Distribution and trends in Arctic sea ice age through spring 2011. Geophysical Research Letters 38, L13502. http://dx.doi.org/10.1029/2011gl047735.

Mathis, J.T., Bates, N.R., Hansell, D.A., Babila, T., 2009. Net community production in the northeastern Chukchi Sea. Deep-Sea Res. II 56, 1213–1222. http://dx.doi.org/10.1016/j.dsr2.2008.10.017.

Mathis, J.T., Cross, J.N., Bates, N.R., 2011. Coupling primary production and terrestrial runoff to ocean acidification and carbonate mineral suppression in the eastern Bering Sea. J. Geophys. Res.-Oceans 116, C02030. http://dx.doi.org/10.1029/2010jc006453.

McLaughlin, F.A., Carmack, E.C., 2010. Deepening of the nutricline and chlorophyll maximum in the Canada Basin interior, 2003–2009. Geophys. Res. Lett. 37, L24602. http://dx.doi.org/10.1029/2010gl045459.

McLaughlin, F.A., Carmack, E.C., Zimmerann, S., Sieberd, G., White, L., Barwell-Clarke, J., Steel, M., Li, W.K., 2008. Physical and chemical data from the Canada Basin, August 2004. Can. Data Rep. Hydrogr. Ocean Sci. 140.

McLaughlin, F., Carmack, E., Proshutinsky, A., Krishfield, R.A., Guay, C., Yamamoto-Kawai, M., Jackson, J.M., Williams, B., 2011. The rapid response of the Canada Basin to climate forcing from bellweather to alarm bells. Oceanography 24, 146–159.

McPhee, M.G., Proshutinsky, A., Morison, J.H., Steele, M., Alkire, M.B., 2009. Rapid change in freshwater content of the Arctic Ocean. Geophys. Res. Lett. 36, L10602. http://dx.doi.org/10.1029/2009gl037525.

Millero, F.J., Poisson, A., 1981. International one-atmosphere equation of state of seawater. Deep-Sea Res. Part A-Oceanogr. Res. Pap. 28, 625–629.

Monier, A., Terrado, R., Thaler, M., Comeau, A., Medrinal, E., Lovejoy, C., 2013. Upper Arctic Ocean water masses harbor distinct communities of heterotrophic flagellates. Biogeosciences 10, 4273–4286. http://dx.doi.org/10.5194/bg-10-4273-2013.

Moran, X.A.G., Lopez-Urrutia, A., Calvo-Diaz, A., Li, W.K.W., 2010. Increasing importance of small phytoplankton in a warmer ocean. Glob. Chang. Biol. 16, 1137–1144. http://dx.doi.org/10.1111/j.1365-2486.2009.01960.x.

Nguyen, D., Maranger, R., Tremblay, J.E., Gosselin, M., 2012. Respiration and bacterial carbon dynamics in the Amundsen Gulf, western Canadian Arctic. J. Geophys. Res.-Oceans 117, C00g16. http://dx.doi.org/10.1029/2011jc007343.

Nicholson, D.P., Stanley, R.H.R., Barkan, E., Karl, D.M., Luz, B., Quay, P.D., Doney, S.C., 2012. Evaluating triple oxygen isotope estimates of gross primary production at the Hawaii Ocean Time-series and Bermuda Atlantic Time-series Study sites. J. Geophys. Res.-Oceans 117, C05012. http://dx.doi.org/10.1029/2010JC006856.

Nicholson, D., Stanley, R.H.R., Doney, S.C., 2014. The triple oxygen isotope tracer of primary productivity in a dynamic ocean. Glob. Biogeochem. Cycles (in press).

Nishino, S., Kikuchi, T., Yamamoto-Kawai, M., Kawaguchi, Y., Hirawake, T., Itoh, M., 2011. Enhancement/reduction of biological pump depends on ocean circulation in the sea-ice reduction regions of the Arctic Ocean. J. Oceanogr. 67, 305–314. http://dx.doi.org/10.1007/s10872-011-0030-7.

Pabi, S., van Dijken, G.L., Arrigo, K.R., 2008. Primary production in the Arctic Ocean, 1998–2006. J. Geophys. Res.-Oceans 113.

Pickart, R.S., Schulze, L.M., Moore, G.W.K., Charette, M.A., Arrigo, K.R., van Dijken, G., Danielson, S.L., 2013. Long-term trends of upwelling and impacts on primary productivity in the Alaskan Beaufort Sea. Deep-Sea Res. Part I-Oceanogr. Res. Pap. 79, 106–121. http://dx.doi.org/10.1016/j.dsr.2013.05.003.

Popova, E.E., Yool, A., Coward, A.C., Dupont, F., Deal, C., Elliott, S., Hunke, E., Jin, M.B., Steele, M., Zhang, J.L., 2012. What controls primary production in the Arctic Ocean? Results from an intercomparison of five general circulation models with biogeochemistry. J. Geophys. Res.-Oceans 117, C00d12. http://dx.doi.org/10.1029/2011jc007112.

Prokopenko, M.G., Pauluis, O.M., Granger, J., Yeung, L.Y., 2011. Exact evaluation of gross photosynthetic production from the oxygen triple-isotope composition of O_2: implications for the net-to-gross primary production ratios. Geophys. Res. Lett. 38 (doi: L1460310.1029/2011gl047652).

Proshutinsky, A., Krishfield, R., Timmermans, M.L., Toole, J., Carmack, E., McLaughlin, F., Williams, W.J., Zimmermann, S., Itoh, M., Shimada, K., 2009. Beaufort Gyre freshwater reservoir: state and variability from observations. J. Geophys. Res.-Oceans 114, C00a10. http://dx.doi.org/10.1029/2008jc005104.

Quay, P.D., Peacock, C., Bjorkman, K., Karl, D.M., 2010. Measuring primary production rates in the ocean: enigmatic results between incubation and non-incubation methods at Station ALOHA. Glob. Biogeochem. Cycles 24. http://dx.doi.org/10.1029/2009GB003665.

Quay, P., Stutsman, J., Steinhoff, T., 2012. Primary production and carbon export rates across the subpolar N. Atlantic Ocean basin based on triple oxygen isotope and dissolved O_2 and Ar gas measurements. Glob. Biogeochem. Cycles 26, Gb2003. http://dx.doi.org/10.1029/2010gb004003.

Reigstad, M., Carroll, J., Slagstad, D., Ellingsen, I., Wassmann, P., 2011. Intra-regional comparison of productivity, carbon flux and ecosystem composition within the northern Barents Sea. Prog. Oceanogr. 90, 33–46. http://dx.doi.org/10.1016/j.pocean.2011.02.005.

Reuer, M.K., Barnett, B.A., Bender, M.L., Falkowski, P.G., Hendricks, M.B., 2007. New estimates of Southern Ocean biological production rates from O_2/Ar ratios and the triple isotope composition of O_2. Deep-Sea Res. Part I-Oceanogr. Res. Pap. 54, 951–974.

Robinson, C., Tilstone, G.H., Rees, A.P., Smyth, T.J., Fishwick, J.R., Tarran, G.A., Luz, B., Barkan, E., David, E., 2009. Comparison of in vitro and in situ plankton production determinations. Aquat. Microb. Ecol. 54, 13–34.

Schulze, L.M., Pickart, R.S., 2012. Seasonal variation of upwelling in the Alaskan Beaufort Sea: impact of sea ice cover. J. Geophys. Res.-Oceans 117 (doi: C06022.10.1029/2012jc007985).

Slagstad, D., Ellingsen, I.H., Wassmann, P., 2011. Evaluating primary and secondary production in an Arctic Ocean void of summer sea ice: an experimental simulation approach. Prog. Oceanogr. 90, 117–131. http://dx.doi.org/10.1016/j.pocean.2011.02.009.

Spitzer, W.S., Jenkins, W.J., 1989. Rates of vertical mixing, gas-exchange and new production — estimates from seasonal gas cycles in the upper ocean near Bermuda. J. Mar. Res. 47, 169–196.

Stanley, R.H.R., Jenkins, W.J., Doney, S.C., Lott III, D.E., 2009. Noble gas constraints on air–sea gas exchange and bubble fluxes. J. Geophys. Res.-Oceans 114. http://dx.doi.org/10.1029/2009JC005396.

Stanley, R.H.R., Kirkpatrick, J.B., Barnett, B., Cassar, N., Bender, M.L., 2010. Net community production and gross production rates in the Western Equatorial Pacific. Glob. Biogeochem. Cycles 24, GB4001 (doi:4010.1029/2009GB003651).

Stroeve, J.C., Serreze, M.C., Holland, M.M., Kay, J.E., Malanik, J., Barrett, A.P., 2012. The Arctic's rapidly shrinking sea ice cover: a research synthesis. Clim. Change 110, 1005–1027. http://dx.doi.org/10.1007/s10584-011-0101-1.

Terrado, R., Lovejoy, C., Massana, R., Vincent, W.F., 2008. Microbial food web responses to light and nutrients beneath the coastal Arctic Ocean sea ice during the winter–spring transition. J. Mar. Syst. 74, 964–977. http://dx.doi.org/10.1016/j.jmarsys.2007.11.001.

Thiemens, M.H., Jackson, T., Zipf, E.C., Erdman, P.W., Vanegmond, C., 1995. Carbon-dioxide and oxygen-isotope anomalies in the mesosphere and stratosphere. Science 270, 969–972.

Tremblay, J.E., Michel, C., Hobson, K.A., Gosselin, M., Price, N.M., 2006. Bloom dynamics in early opening waters of the Arctic Ocean. Limnol. Oceanogr. 51, 900–912.

Tremblay, J.E., Simpson, K.G., Martin, J., Miller, L., Gratton, Y., Barber, D., Price, N.M., 2008. Vertical stability and the annual dynamics of nutrients and chlorophyll fluorescence in the coastal, southeast Beaufort Sea. J. Geophys. Res.-Oceans 113, C07s90. http://dx.doi.org/10.1029/2007jc004547.

Tremblay, J.E., Belanger, S., Barber, D.G., Asplin, M., Martin, J., Darnis, G., Fortier, L., Gratton, Y., Link, H., Archambault, P., Sallon, A., Michel, C., Williams, W.J., Philippe, B., Gosselin, M., 2011. Climate forcing multiplies biological productivity in the coastal Arctic Ocean. Geophys. Res. Lett. 38, L18604. http://dx.doi.org/10.1029/2011gl048825.

Tremblay, J.E., Robert, D., Varela, D.E., Lovejoy, C., Darnis, G., Nelson, R.J., Sastri, A.R., 2012. Current state and trends in Canadian Arctic marine ecosystems: I. Primary production. Clim. Change. http://dx.doi.org/10.1007/s10584-012-0496-3.

Trenberth, K.E., Jones, P.D., Amenhem, P., Bojariu, R., Easterling, D., Tank, A.K., Parker, D., Rahimzadeh, F., Renwick, J.A., Rusticucci, M., Soden, B.J., Zhai, P., 2007. Observations: surface and atmospheric climate change. In: Solomon, S., Qin, D., Manning, M., Chen, Z., Marquis, M., Avery, K.B., Tignor, M., Miller, H.L. (Eds.), Climate change 2007: the physical science basis. Contribution of Working Group I to the Fourth Assessment Report of the Intergovernmental Panel on Climate Change. Cambridge University Press, Cambridge.

Vaquer-Sunyer, R., Duarte, C.M., Santiago, R., Wassmann, P., Reigstad, M., 2010. Experimental evaluation of planktonic respiration response to warming in the European Arctic Sector. Polar Biol. 33, 1661–1671. http://dx.doi.org/10.1007/s00300-010-0788-x.

Vaquer-Sunyer, R., Duarte, C.M., Regaudie-de-Gioux, A., Holding, J., Garcia-Corral, L.S., Reigstad, M., Wassmann, P., 2013. Seasonal patterns in Arctic planktonic metabolism (Fram Strait — Svalbard region). Biogeosciences 10, 1451–1469. http://dx.doi.org/10.5194/bg-10-1451-2013.

Wassmann, P., 2011. Arctic marine ecosystems in an era of rapid climate change. Prog. Oceanogr. 90, 1–17. http://dx.doi.org/10.1016/j.pocean.2011.02.002.

Wassmann, P., Slagstad, D., Ellingsen, I., 2010. Primary production and climatic variability in the European sector of the Arctic Ocean prior to 2007: preliminary results. Polar Biol. 33, 1641–1650. http://dx.doi.org/10.1007/s00300-010-0839-3.

Wassmann, P., Duarte, C.M., Agusti, S., Sejr, M.K., 2011. Footprints of climate change in the Arctic marine ecosystem. Glob. Chang. Biol. 17, 1235–1249. http://dx.doi.org/10.1111/j.1365-2486.2010.02311.x.

WMO, 1989. WMO Sea-ice Nomenclature. In: Organization W.M. (Ed.), p. 145 (Supplement No. 5).

Worby, A.P., Allison, I., 1999. A technique for making ship-based observations of Antarctic sea ice thickness and characteristics, part I: Observational technique and results. In: Worby, A.P. (Ed.), Observing Antarctic Sea Ice: A Practical Guide for Conducting Sea Ice Observations from Vessels Operating in the Antarctic Pack Ice. Sci. Comm. Antarct. Res. Hobart, Tasmania, Australia.

Yamamoto-Kawai, M., McLaughlin, F.A., Carmack, E.C., Nishino, S., Shimada, K., Kurita, N., 2009. Surface freshening of the Canada Basin, 2003–2007: river runoff versus sea ice meltwater. J. Geophys. Res.-Oceans 114, C00a05. http://dx.doi.org/10.1029/2008jc005000.

Yamamoto-Kawai, M., McLaughlin, F.A., Carmack, E.C., 2011. Effects of ocean acidification, warming and melting of sea ice on aragonite saturation of the Canada Basin surface water. Geophys. Res. Lett. 38 (doi: L0360110.1029/2010gl045501).